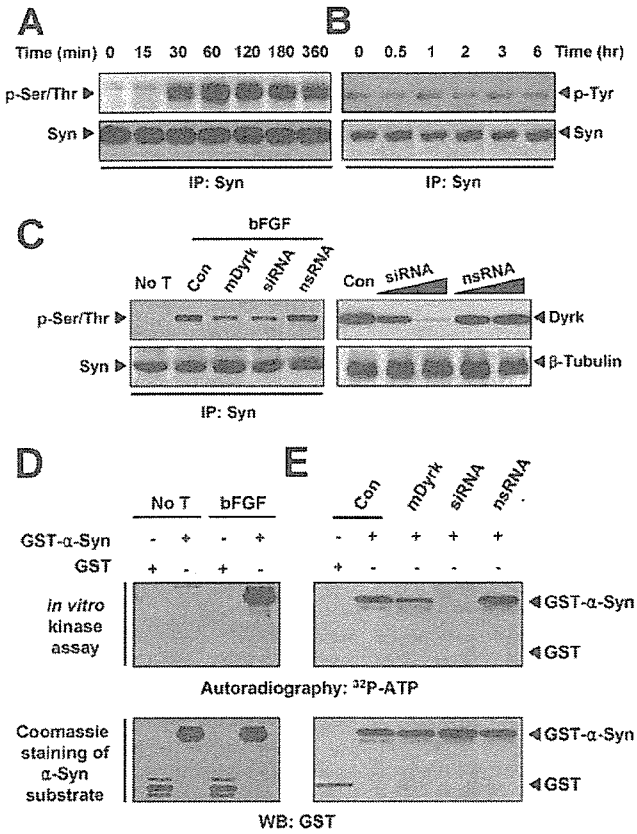

FIGURE 3. **Active Dyrk1A phosphorylates α-synuclein *in vivo* and *in vitro*.** *A*, H19-7 cells were transiently transfected with α-synuclein for 24 h and stimulated with bFGF for the indicated times in differentiation conditions. Immunoprecipitation was performed with anti-α-synuclein (*Syn*) antibody, and the immunocomplexes were analyzed by Western blotting (*WB*) with either anti-α-synuclein or phosphoserine/phosphothreonine (*p-Ser/Thr*) antibodies. *B*, as performed in *A*, except using phosphotyrosine (*p-Tyr*) antibodies. *C*, H19-7 cells were transiently transfected with α-synuclein plasmid alone (*No T* or *Con*) or together with a kinase-deficient Dyrk1A (*mDyrk*). Where indicated, α-synuclein was co-transfected with either silencing Dyrk1A siRNA (*siRNA*) or noncompetitive control siRNA (*nsRNA*). After 24 h, cells were left untreated (*No T*) or stimulated with bFGF for 1 h. Immunoprecipitation was performed with anti-α-synuclein IgG. Immunocomplexes were examined by Western analysis with anti-phosphoserine/phosphothreonine antibodies (*left*). The blocking of Dyrk1A expression by siRNA was determined by Western blotting with anti-Dyrk1A antibodies (*right*). β-Tubulin expression showed equal loading. *D*, H19-7 cells were either untreated or stimulated with bFGF for 1 h under differentiation conditions, and cell lysates were immunoprecipitated with anti-Dyrk1A antibodies. By using anti-Dyrk1A immunocomplexes, *in vitro* kinase was performed with either GST or GST fused with α-synuclein (*GST-Syn*) protein as a substrate. Phosphorylated GST-α-synuclein levels were visualized by autoradiography (*Ag*) (*top*). The purity of each GST or GST-α-synuclein was assayed by Western blot with anti-GST IgG (*bottom*). *E*, H19-7 cells were mock-transfected (*Con*) or transfected with kinase-defective Dyrk1A, competitive (siRNA), or noncompetitive siRNA for 24 h, and stimulated with bFGF for 1 h. After, Dyrk1A was immunoprecipitated for an *in vitro* kinase assay using α-synuclein as a substrate. These results are representative of two or three independent experiments.

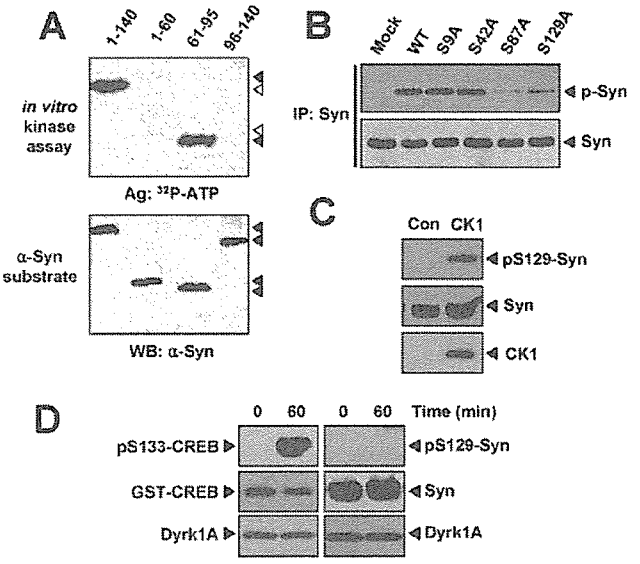

FIGURE 4. **Dyrk1A selectively phosphorylates α-synuclein at the Ser-87 residue.** *A*, four recombinant α-synuclein proteins, full length (residues 1–140), amphipathic N-terminal region (residues 1–60), NAC region (residues 61–95), or C-terminal acidic tail region (residues 96–140) were tested for phosphorylation by immunoprecipitated Dyrk1A (*top*). Dyrk1A was immunoprecipitated from differentiating H19-7 cells. Only two α-synuclein recombinant proteins were phosphorylated (*filled arrowhead*). The *bottom panel* shows input recombinant α-synuclein proteins via Western blot analysis. *B*, H19-7 cells were mock-transfected or transfected for 24 h with α-synuclein wild type or point mutants, S4A, S42A, S87A, and S129A. After 1 h of bFGF stimulation in differentiation conditions, cell lysates were prepared and immunoprecipitated (*IP*) with anti-synuclein (*Syn*) IgG, followed by immunoblotting with either anti-α-synuclein or anti-phosphoserine/phosphothreonine (*p-S/T*) antibodies. These results are representative of two independent experiments. *C*, the recombinant α-synuclein has been incubated with *in vitro* phosphorylation system in the absence or presence of casein kinase 1 (*CK1*) for 3 h. The occurrence of α-synuclein phosphorylation at Ser-129 has been examined by immunoblotting with anti-PSer-129 antibody. *D*, cells were transfected with Dyrk1A for 24 h, and cell lysates were immunoprecipitated with anti-Dyrk1A IgG. *In vitro* phosphorylation by anti-Dyrk1A immunocomplexes was performed with either GST-CREB or recombinant α-synuclein as a substrate. The phosphorylation of CREB at Ser-133 or α-synuclein at Ser-129 was determined by immunoblotting with their specific antibodies, as indicated.

Next, we asked if endogenous Dyrk1A interacts with α-synuclein in the mammalian central nervous systems. α-Synuclein and Dyrk1A are highly expressed in rat brain lysates and primary cortical neurons (Fig. 2, *A* and *B*). As shown in Fig. 2, α-synuclein selectively associates with Dyrk1A, and we did not observe nonspecific interaction with preimmune IgG or protein A beads (Fig. 2, *A* and *B*). Moreover, immunostaining of primary cortical neurons showed that Dyrk1A and α-synuclein co-localize in the cytoplasm (Fig. 2*C*). These data suggest that the Dyrk1A and α-synuclein interaction is not an artifact observed in transformed cell lines but occurs in the mammalian central nervous system.

Dyrk1A Phosphorylates α-Synuclein upon the Stimulation with bFGF in H19-7 Cells—Previously, we showed that basic fibroblast growth factor (bFGF) addition to H19-7 cells causes Dyrk1A activation, which plays an important role during neuronal differentiation of H19-7 cells (21). Based on these findings, we tested whether active Dyrk1A directly phosphorylates α-synuclein. Transient α-synuclein expression in H19-7 cells, followed by bFGF stimulation under the neuronal differentiation conditions, enhanced Ser/Thr phosphorylation within 6 h, reaching a maximum at 1 h (Fig. 3*A*). Since Dyrk1A acts as a dual specificity protein kinase, which catalyzes the tyrosine-directed autophosphorylation as well as serine/threonine residue phosphorylation in exogenous substrates (27), α-synuclein could also be phosphorylated at tyrosine residues. We performed a similar experiment to determine whether α-synuclein was phosphorylated on tyrosine residue(s). As shown in Fig. 3*B*,

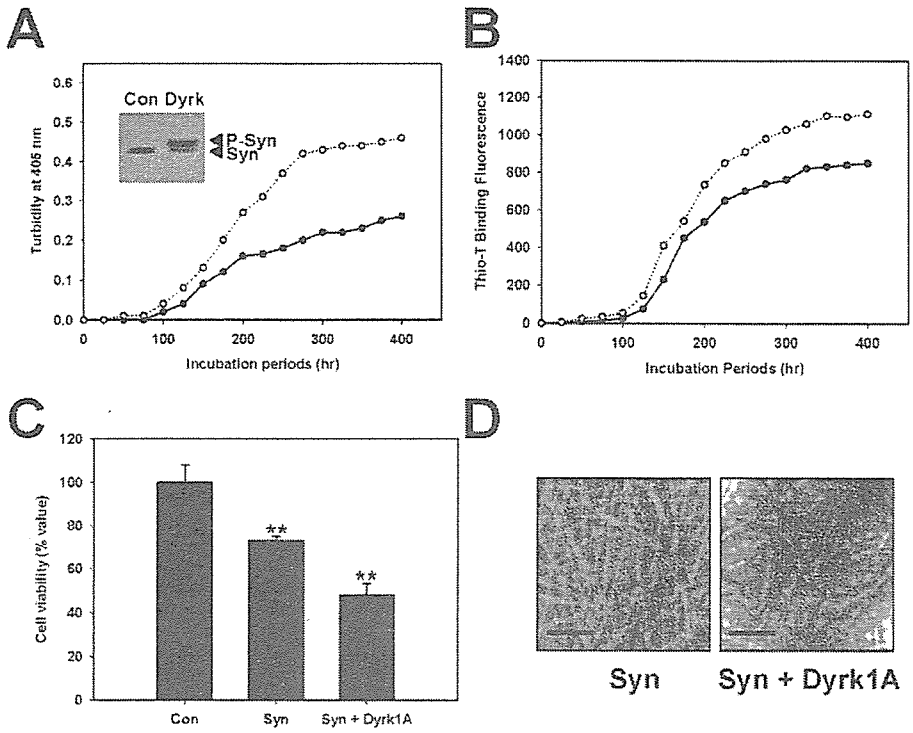

FIGURE 5. **Dyrk1A-induced α-synuclein phosphorylation promotes intracellular inclusion formation and increases cytotoxicity.** Aggregation kinetics of intact α-synuclein or phosphorylated proteins by active Dyrk1A immunocomplexes was evaluated with turbidity (*A*) and thioflavin-T binding fluorescence (*B*). α-Synuclein protein aggregations were performed using α-synuclein (50 μg) with or without active Dyrk1A immunoprecipitates (~0.4 μg). Turbidity (*A*) and amyloid formation (*B*) in the presence (*open circles*) and absence (*closed circles*) of anti-Dyrk1A immunocomplexes were measured by absorbance at 405 nm and thioflavin-T binding fluorescence. The proteins were immunoblotted with anti-α-synuclein antibody to analyze for α-synuclein phosphorylation by a gel shift assay in the *inset* (*A*). Intact α-synuclein (*Syn*) and its phosphorylated bands (*P-Syn*) are indicated with *arrows*. *C*, cell viability was measured by the 3-(4,5-dimethylthiazol-2-yl)-2,5-diphenyltetrazolium bromide extract assay, after treatment with either intact α-synuclein aggregate (*Syn*) or the α-synuclein aggregate incubated with active Dyrk1A immunocomplexes (*Syn + Dyrk1A*) (**, $p < 0.01$ *versus* control). *D*, α-Synuclein aggregate morphological differences were examined. α-Synuclein aggregates prepared in the absence (*Syn*) or the presence of bFGF-induced active Dyrk1A (*Syn + Dyrk1A*) were examined by electron microscopy (magnification, ×78,000). *Scale bars*, 0.5 μm. These results are representative of two or three independent experiments.

we did not detect tyrosine-phosphorylated α-synuclein within 6 h of bFGF treatment, in H19-7 cells.

To clarify whether α-synuclein phosphorylation is due to active Dyrk1A, we tested whether a kinase-deficient Dyrk1A mutant or Dyrk1A siRNA duplex affects α-synuclein phosphorylation. As shown in Fig. 3*C*, α-synuclein phosphorylation was significantly diminished by expressing a kinase-dead Dyrk1A mutant and Dyrk1A siRNA, as compared with control cells. As a negative control, the transient expression of nonsilencing siRNAs did not affect α-synuclein phosphorylation (Fig. 3*C*). As expected, the Dyrk1A siRNA duplex, but not nonspecific siRNAs, blocked the endogenous Dyrk1A expression in a dose-dependent manner (Fig. 3*C*).

To verify the specific role of Dyrk1A on α-synuclein phosphorylation, we utilized an *in vitro* kinase assay. We used immunoprecipitated Dyrk1A, from H19-7 cells, to phosphorylate recombinant α-synuclein (GST-α-synuclein). As shown in Fig. 3*D*, the serine/threonine phosphorylation(s) of α-synuclein was significantly enhanced upon bFGF stimulation. As a control, GST alone was not phosphorylated by anti-Dyrk1A immunocomplexes (Fig. 3*D*). Furthermore, anti-Dyrk1A immunocomplexes prepared after α-synuclein transfection with either kinase-inactive Dyrk1A or competitive Dyrk1A siRNAs significantly reduced α-synuclein phosphorylation (Fig. 3*E*). Transient, non-competitive Dyrk1A siRNAs had no effect on α-synuclein phosphorylation (Fig. 3*E*). Taken together, these data suggest that active Dyrk1A selectively phosphorylates α-synuclein at serine/threonine residue(s).

Dyrk1A Phosphorylates Ser-87 Residue within α-Synuclein—To identify the specific α-synuclein residues phosphorylated by Dyrk1A, we used recombinant α-synuclein fragments as substrates for an *in vitro* kinase assay. As shown in Fig. 4*A*, active Dyrk1A phosphorylated α-synuclein peptides consisting of amino acids 1–140 and 61–95. However, Dyrk1A did not phosphorylate the C-terminal peptide (residues 96–140) or the N-terminal peptide (residues 1–60) (Fig. 4*A*), suggesting that the critical phosphorylated amino acid(s) resided between amino acids 61 and 95. Sequence analysis identified four possible phosphorylatable serines at positions 9, 42, 87, and 129. Therefore, we hypothesized that Dyrk1A phosphorylated α-synuclein at serine 87. To test this hypothesis, we mutated each serine residue (positions 9, 42, 87, and 129) to an alanine and examined α-synuclein phosphorylation after bFGF stimulation. The α-synuclein mutants S9A and S42A were readily phosphorylated in response to bFGF-induced active Dyrk1A, indicating that these residues were probably not involved in Dyrk1A-mediated phosphorylation (Fig. 4*B*). However, when cells were transfected with the α-synuclein S87A mutant, bFGF-induced α-synuclein phosphorylation was abolished (Fig. 4*B*). Interestingly, the α-synuclein S129A also blocked α-synuclein phosphorylation (Fig. 4*B*), suggesting that active Dyrk1A selectively phosphorylates α-synuclein at the serine 87 residue, whereas neurogenic bFGF appears to activate other protein kinase(s) to modify α-synuclein at the serine 129 residue. This finding was further confirmed by using the antibody against phospho-Ser-129-α-synuclein (PSer-129). Based on our previous finding (13), PSer-129 antibody was first verified by *in vitro* phosphorylation of α-synuclein by casein kinase 1 (Fig. 4*C*). Then active Dyrk1A immunocomplexes, which were validated through CREB phosphorylation at Ser-133 *in vitro* (21), was shown not to phosphorylate α-synuclein at Ser-129 (Fig. 4*D*).

The Kinetics and Neurotoxicity Induced by Intact α-Synuclein Inclusions Are Different from the Phosphorylated Forms by Dyrk1A—We monitored protein aggregation of recombinant or phosphorylated wild type α-synuclein samples by measuring

the turbidity (Fig. 5A). As monitored by UV absorption at 280 nm, incubating purified α-synuclein at 37 °C led to insoluble aggregate formation. Phosphorylated α-synuclein exhibited more aggressive aggregate formation as compared with unphosphorylated, wild type α-synuclein (Fig. 5A). Measurement of thioflavin-T binding fluorescence confirmed that phosphorylated α-synuclein exhibited enhanced aggregation as compared with unphosphorylated α-synuclein, although the difference was not as large as observed in the turbidity measurements (Fig. 5B).

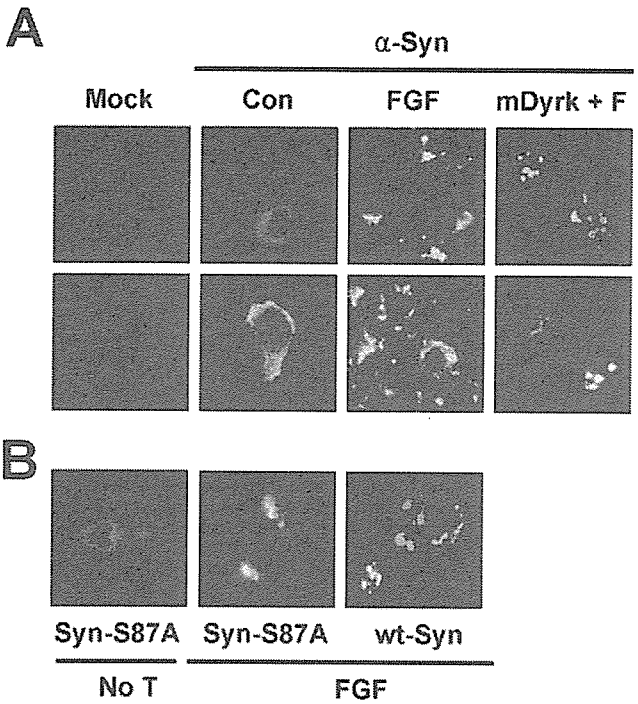

FIGURE 6. **α-Synuclein phosphorylation at Ser-87 by Dyrk1A enhances aggregate formation and neuronal cell death in H19-7 cells.** *A*, cells were mock-transfected (*Mock*) or transfected with α-synuclein alone or transfected with α-synuclein and kinase-defective Dyrk1A plasmid (*mDyrk*) for 24 h. Cells were untreated (*Mock*, *Con*) or stimulated with bFGF (*bFGF* or *F*) for 48 h. Immunocytochemical analysis was performed with anti-α-synuclein antibodies. Representative images of cells expressing α-synuclein are shown by confocal microscopy. *B*, cells were transfected with either wild type α-synuclein (*wt-Syn*) or α-synuclein S87A mutant (*Syn-S87A*) for 24 h and left untreated (*No T*) or stimulated with bFGF for 48 h. These data are representative of three independent experiments.

We next asked whether the enhanced aggregation of phosphorylated α-synuclein proteins exhibited greater cytotoxicity. Phosphorylated α-synuclein protein aggregates were more cytotoxic than unphosphorylated α-synuclein aggregates (Fig. 5C). Transmission electron microscopy analysis of the aggregated granular structure formation during the α-synuclein aggregation in the presence of protein phosphorylation was microscopically distinct from those aggregates from unphosphorylated α-synuclein (Fig. 5D). Intact α-synuclein aggregates contained only the fibrillar forms, whereas the inclusions obtained with the Dyrk1A-induced phospho-α-synuclein showed that spherical granular forms are also present, in addition to the fibrillar aggregates (Fig. 5D).

The α-Synuclein Phosphorylation via Active Dyrk1A Promotes Intracellular α-Synuclein Inclusion Formation—To validate the consequences of α-synuclein Ser-87 phosphorylation, we tested whether Dyrk1A could influence the insoluble α-synuclein aggregate formation, in H19-7 cells. Previously, we showed that transient α-synuclein expression in H19-7 cells leads to neuronal cell death. This effect is closely associated with the formation of intracytoplasmic α-synuclein-positive inclusions, which have similar composition to LBs found in PD patients (26). After H19-7 cells were transfected with α-synuclein, the expression pattern of α-synuclein within the cells was compared in the absence or presence of bFGF. Consistent with our previous finding, the distribution of α-synuclein was uneven and took the form of granular aggregates (Fig. 6A). Stimulation with bFGF enhanced intracytoplasmic α-synuclein inclusion formation (Fig. 6A). Additionally, α-synuclein co-expression with the dominant negative Dyrk1A diminished α-synuclein aggregates, as compared with α-synuclein alone (Fig. 6A). Cells expressing the α-synuclein S87A mutant also exhibited reduced aggregate formation (Fig. 6B). Quantification of intracellular eosinophilic protein aggregates found a 2-fold increase when cells were transfected with α-synuclein plus GFP and stimulated with bFGF (Table 1). However, we did not observe this increase in cells transfected with either α-synuclein S87A or kinase-deficient Dyrk1A in the absence of bFGF stimuli (Table 1).

Following transient α-synuclein expression, we measured cell viability after 24 h. As shown in Table 1, α-synuclein overexpression significantly decreased the cell viability by ~42% in H19-7 cells. Consistent with a previous report that H19-7 cells

TABLE 1

α-Synuclein phosphorylation effects on cell viability and eosinophilic inclusion formation in hippocampal H19-7 cells

Cells were transfected and then left untreated or stimulated with bFGF under neuronal differentiation conditions, as indicated. WT, wild type; Syn, synuclein.

Treatment	Transfection	GFP-expressing cells with hematoxylin and eosin-positive inclusions[a]	Cell viability[b]
		%	%
None	GFP	ND[c]	100 ± 0.7
	GFP + WT Syn	28.1 ± 2.6	58.1 ± 3.9
	GFP + Syn S87A	16.9 ± 1.8	77.2 ± 4.5
	GFP + WT Syn + mDyrk1A	11.8 ± 1.6	83.3 ± 2.6
bFGF	GFP	ND	75.4 ± 3.4
	GFP + WT Syn	51.9 ± 5.5[d]	41.2 ± 4.9[d]
	GFP + Syn S87A	26.7 ± 2.9[d]	72.4 ± 3.5[d]
	GFP + WT Syn + mDyrk1A	22.2 ± 1.6[d]	68.2 ± 3.8[d]

[a] Number of GFP-positive cells containing eosinophilic inclusions was counted in six different fields among approximately 250 cells/experimental condition. Data are shown as the means ± S.E. from three separate experiments performed in duplicate (**, $p < 0.01$ *versus* cells transfected with wild type α-synuclein alone).
[b] Cell viability was measured by the tetrazolium salt, 3-(4,5-dimethylthiazol-2-yl)-2,5-diphenyltetrazolium bromide extraction method.
[c] ND, not determined.
[d] $p < 0.01$ *versus* cells transfected with wild type α-synuclein alone.

also undergo apoptosis upon differentiation (28), bFGF addition resulted in a 25% loss of the total cell population, within 24 h (Table 1). However, co-transfection with wild type α-synuclein plus dominant-negative Dyrk1A diminished the neuronal cell death (Table 1). Furthermore, when cells were transfected with α-synuclein S87A, cytotoxicity was significantly reduced in response to bFGF. As a control, transfection of either kinase-dead Dyrk1A or α-synuclein S87A mutant in the absence of fibroblast growth factor stimulation reduced the toxic effect (Table 1). These data indicate that active Dyrk1A increases intracellular α-synuclein aggregates and potentiates its cytotoxicity in H19-7 cells.

DISCUSSION

Several examples of α-synuclein post-translational modifications have been reported in the human brain, including phosphorylation (14), nitration (29), glycosylation (30), and SUMO modification (31). α-Synuclein phosphorylation reduces lipid binding and enhances fibril formation (15). Supporting this finding, phosphorylated forms of α-synuclein at its Ser-129 and Ser-87 residues are found in LBs (13). Furthermore, α-synuclein post-translational modifications by tyrosine nitration and oxidation can also promote intracytoplasmic inclusion formation (32, 33).

α-Synuclein can be phosphorylated *in vitro* at several residues, including serines 87 and 129 and three C-terminal tyrosine residues (tyrosines 125, 133, and 136). Several protein kinases were reported to phosphorylate α-synuclein *in vitro* and/or *in vivo*. For example, G protein-coupled receptor kinase-2 phosphorylates Ser-129 *in vivo* and enhances α-synuclein toxicity (16). Casein kinase 1 and 2 can also phosphorylate Ser-129 of α-synuclein in cultured cells (13). In addition, the α-synuclein Tyr-125 residue is phosphorylated by c-Src and Fyn (34, 35). Although α-synuclein is constitutively phosphorylated at Ser-87 as well as at Ser-129 residues (13), the kinase targeting serine 87 residue and its physiological role have not been described. We examined whether α-synuclein is a Dyrk1A phosphorylation target. The current study shows that Dyrk1A can phosphorylate α-synuclein at Ser-87, and this enhances cytoplasmic aggregate formation. In addition to Ser-129, the Ser-87 residue plays an important role modulating cytoplasmic α-synuclein inclusion formation. Dyrk1A catalyzes the tyrosine-directed autophosphorylation and serine/threonine phosphorylation in exogenous substrates (27). Therefore, we could not exclude the possibility that Dyrk1A can phosphorylate α-synuclein at tyrosine residues. Western blot analysis of anti-α-synuclein immunocomplexes with anti-phosphotyrosine IgGs revealed that the tyrosine residues within the α-synuclein are not probably phosphorylated in response to bFGF-induced active Dyrk1A, in H19-7 cells.

Previously, we reported that active Dyrk1A phosphorylates CREB, which subsequently leads to the stimulation of cAMP-response element-mediated gene transcription, during neuronal differentiation (21). These data strongly suggest that Dyrk1A may play an important role during the neurogenic factor-induced differentiation of central nervous system neuronal cells. In addition, our recent findings show that huntingtin-interacting protein-1 phosphorylation by Dyrk1A has an important role in neuronal differentiation and cell death (36). The present study demonstrates that α-synuclein is a Dyrk1A phosphorylation target, and this modification results in enhanced aggregate formation, which potentiates the proapoptotic effects of α-synuclein. Supporting our current findings are other reports that show that Dyrk1A phosphorylates human microtubule-associated tau protein at Thr-212, a residue that is hyperphosphorylated in AD and tauopathies (37). Abnormally increased Dyrk1A immunoreactivity is found in AD and DS (38), suggesting a possible involvement of Dyrk1A with neurofibrillary tangle pathology.

Through the aggregation assay *in vitro*, we observed the generation of previously unrecognized positive regulation of α-synuclein aggregation through protein phosphorylation. The aggregation of α-synuclein in the unstimulated quiescent condition can be positively regulated by active Dyrk1A. In addition, electron microscopy shows the aggregates prepared from phosphorylated α-synuclein protein have a globular protofibrillar structure quite distinct from the fibril forming from intact α-synuclein. Caughey and Lansbury (39) and Lansbury *et al.* (40) demonstrated that *in vitro* fibril formation by α-synuclein from its soluble monomeric form does not follow a simple one-step transition but is a rather complex process involving one or more discrete intermediates, termed protofibrils. During the process, a protofibril intermediate rather than the fibril itself may be more pathogenic. Additionally, studies have characterized several α-synuclein oligomers, which are much smaller than fibrils and appear early in the fibrillization process as granular forms (39, 40). Consistent with this view, the morphological difference between the two protein aggregations is reflected by their distinct aggregation patterns, kinetics, and neurotoxicity. Further studies to characterize the molecular mechanisms leading to intracellular α-synuclein aggregate formation as well as the important signal transduction pathway(s) will give us insight into the mechanism of LB formation and the pathogenesis of PD and DS.

Acknowledgments—We are deeply grateful to W. Becker, R. Jakes, C. A. Ross, and J. L. Benovic for generously providing cDNA constructs and to H. J. Cho and J. Y. Yang for technical assistance.

REFERENCES

1. Spillantini, M. G., and Goedert, M. (2000) *Ann. N. Y. Acad. Sci.* **920**, 16–27
2. Hashimoto, M., Kawahara, K., Bar-On, P., Rockenstein, E., Crews, L., and Masliah, E. (2004) *J. Mol. Neurosci.* **24**, 343–352
3. Yoshimoto, M., Iwai, A., Kang, D., Otero, D. A., Xia, Y., and Saitoh, T. (1995) *Proc. Natl. Acad. Sci. U. S. A.* **92**, 9141–9145
4. Cookson, M. R. (2005) *Annu. Rev. Biochem.* **74**, 29–52
5. Lejeune, J., Turpin, R., and Gautier, M. (1959) *Bull. Acad. Natl. Med.* **143**, 256–265
6. Korenberg, J. R., Chen, X. N., Schipper, R., Sun, Z., Gonsky, R., Gerwehr, S., Carpenter, N., Daumer, C., Dignan, P., Disteche, C., Graham, J. M., Hugdins, L., McGillivray, B., Miyazaki, K., Ogasawara, N., Park, J. P., Pagon, R., Pueschel, S., Sack, G., Say, B., Schuffenhauer, S., Soukup, S., and Yamanaka, T. (1994) *Proc. Natl. Acad. Sci. U. S. A.* **91**, 4997–5001
7. Patterson, D. (1987) *Sci. Am.* **257**, 52–57
8. Pulsifer, M. B. (1996) *J. Int. Neuropsychol. Soc.* **2**, 159–176
9. Guimera, J., Casas, C., Estivill, X., and Pritchard, M. (1999) *Genomics* **57**, 407–418
10. Kentrup, H., Becker, W., Heukelbach, J., Wilmes, A., Schurmann, A.,

Huppertz, C., Kainulainen, H., and Joost, H. G. (1996) *J. Biol. Chem.* **271,** 3488–3495
11. Guimera, J., Casas, C., Pucharcos, C., Solans, A., Domenech, A., Planas, A. M., Ashley, J., Lovett, M., Estivill, X., and Pritchard, M. A. (1996) *Hum. Mol. Genet.* **5,** 1305–1310
12. Altafaj, X., Dierssen, M., Baamonde, C., Marti, E., Visa, J., Guimera, J., Oset, M., Gonzalez, J. R., Florez, J., Fillat, C., and Estivill, X. (2001) *Hum. Mol. Genet.* **10,** 1915–1923
13. Okochi, M., Walter, J., Koyama, A., Nakajo, S., Baba, M., Iwatsubo, T., Meijer, L., Kahle, P. J., and Haass, C. (2000) *J. Biol. Chem.* **275,** 390–397
14. Fujiwara, H., Hasegawa, M., Dohmae, N., Kawashima, A., Masliah, E., Goldberg, M. S., Shen, J., Takio, K., and Iwatsubo, T. (2002) *Nat. Cell Biol.* **4,** 160–164
15. Smith, W. W., Margolis, R. L., Li, X., Troncoso, J. C., Lee, M. K., Dawson, V. L., Dawson, T. M., Iwatsubo, T., and Ross, C. A. (2005) *J. Neurosci.* **25,** 5544–5552
16. Pronin, A. N., Morris, A. J., Surguchov, A., and Benovic, J. L. (2000) *J. Biol. Chem.* **275,** 26515–26522
17. Nakamura, T., Yamashita, H., Takahashi, T., and Nakamura, S. (2001) *Biochem. Biophys. Res. Commun.* **280,** 1085–1092
18. Lippa, C. F., Schmidt, M. L., Lee, V. M., and Trojanowski, J. Q. (1999) *Ann. Neurol.* **45,** 353–357
19. Simard, M., and van Reekum, R. (2001) *Int. J. Geriatr. Psychiatry* **16,** 311–320
20. Kim, S. J., Sung, J. Y., Um, J. W., Hattori, N., Mizuno, Y., Tanaka, K., Paik, S. R., Kim, J., and Chung, K. C. (2003) *J. Biol. Chem.* **278,** 41890–41899
21. Yang, E. J., Ahn, Y. S., and Chung, K. C. (2001) *J. Biol. Chem.* **276,** 39819–39824
22. Yang, E. J., Yoon, J. H., and Chung, K. C. (2004) *J. Biol. Chem.* **279,** 1827–1837
23. Sung, J. Y., Park, S. M., Lee, C. H., Um, J. W., Lee, H. J., Kim, J., Oh, Y. J., Lee, S. T., Paik, S. R., and Chung, K. C. (2005) *J. Biol. Chem.* **280,** 25216–25224
24. Sitz, J. H., Tigges, M., Baumgartel, K., Khaspekov, L. G., and Lutz, B. (2004) *Mol. Cell. Biol.* **24,** 5821–5834
25. Sung, J. Y., Kim, J., Paik, S. R., Park, J. H., Ahn, Y. S., and Chung, K. C. (2001) *J. Biol. Chem.* **276,** 27441–27448
26. Kim J. (1997) *Mol. Cells* **7,** 78–83
27. Galceran, J., de Graaf, K., Tejedor, F. J., and Becker, W. (2003) *J. Neural. Transm. Suppl.* **67,** 139–148
28. Eves, E. M., Boise, L. H., Thompson, C. B., Wagner, A. J., Hay, N., and Rosner, M. R. (1996) *J. Neurochem.* **67,** 1908–1920
29. Giasson, B. I., Duda, J. E., Murray, I. V., Chen, Q., Souza, J. M., Hurtig, H. I., Ischiropoulos, H., Trojanowski, J. Q., and Lee, V. M. (2000) *Science* **290,** 985–989
30. Shimura, H., Schlossmacher, M. G., Hattori, N., Frosch, M. P., Trockenbacher, A., Schneider, R., Mizuno, Y., Kosik, K. S., and Selkoe, D. J. (2001) *Science* **293,** 263–269
31. Dorval, V., and Fraser, P. E. (2006) *J. Biol. Chem.* **281,** 9919–9924
32. Hodara, R., Norris, E. H., Giasson, B. I., Mishizen-Eberz, A. J., Lynch, D. R., Lee, V. M., and Ischiropoulos, H. (2004) *J. Biol. Chem.* **279,** 47746–47753
33. Paik, S. R., Shin, H. J., and Lee, J. H. (2000) *Arch. Biochem. Biophys.* **378,** 269–277
34. Ellis, C. E., Schwartzberg, P. L., Grider, T. L., Fink, D. W., and Nussbaum, R. L. (2001) *J. Biol. Chem.* **276,** 3879–3884
35. Nakamura, T., Yamashita, H., Nagano, Y., Takahashi, T., Avraham, S., Avraham, H., Matsumoto, M., and Nakamura, S. (2002) *FEBS Lett.* **521,** 190–194
36. Kang, J. E., Choi, S. A., Park, J. B., and Chung, K. C. (2005) *J. Neurosci. Res.* **81,** 62–72
37. Woods, Y. L., Cohen, P., Becker, W., Jakes, R., Goedert, M., Wang, X., and Proud, C. G. (2001) *Biochem. J.* **355,** 609–615
38. Ferrer, I., Barrachina, M., Puig, B., Martinez de Lagran, M., Marti, E., Avila, J., and Dierssen, M. (2005) *Neurobiol. Dis.* **20,** 392–400
39. Caughey, B., and Lansbury, P. T. (2003) *Annu. Rev. Neurosci.* **26,** 267–298
40. Conway, K. A., Rochet, J. C., Bieganski, R. M., and Lansbury, P. T. (2001) *Science* **294,** 1346–1349
41. Ueda, K., Fukushima, H., Masliah, E., Xia, Y., Iwai, A., Yoshimoto, M., Otero, D. A., Kondo, J., Ihara, Y., and Saitoh, T. (1993) *Proc. Natl. Acad. Sci. U. S. A.* **90,** 11282–11286

Small Molecule Inhibitors of α-Synuclein Filament Assembly

Masami Masuda, Nobuyuki Suzuki, Sayuri Taniguchi, Takayuki Oikawa, Takashi Nonaka, Takeshi Iwatsubo, Shin-ichi Hisanaga, Michel Goedert, and Masato Hasegawa

Department of Molecular Neurobiology, Tokyo Institute of Psychiatry, 2-1-8 Kamikitazawa, Setagaya-ku, Tokyo 156-8585, Japan, Molecular Neuroscience Laboratory, Graduate School of Science, Tokyo Metropolitan University, 1-1 Minami-Osawa, Hachioji-shi, Tokyo 192-0397, Japan, New Product Research Laboratory II, Daiichi Pharmaceutical Company Ltd., 16-13 Kita-Kasai 1-Chome, Edogawa-ku, Tokyo 134-8630, Japan, Department of Neuropathology and Neuroscience, Graduate School of Pharmaceutical Science, The University of Tokyo, 7-3-1 Hongo, Bunkyo-ku, Tokyo 113-0033, Japan, and Medical Research Council Laboratory of Molecular Biology, Hills Road, Cambridge CB2 2QH, U.K.

Biochemistry®

Reprinted from
Volume 45, Number 19, Pages 6085–6094

Small Molecule Inhibitors of α-Synuclein Filament Assembly†

Masami Masuda,[‡,§] Nobuyuki Suzuki,[∥] Sayuri Taniguchi,[‡,⊥] Takayuki Oikawa,[‡,§] Takashi Nonaka,[‡] Takeshi Iwatsubo,[⊥] Shin-ichi Hisanaga,[§] Michel Goedert,[@] and Masato Hasegawa*[,‡]

Department of Molecular Neurobiology, Tokyo Institute of Psychiatry, 2-1-8 Kamikitazawa, Setagaya-ku, Tokyo 156-8585, Japan, Molecular Neuroscience Laboratory, Graduate School of Science, Tokyo Metropolitan University, 1-1 Minami-Osawa, Hachioji-shi, Tokyo 192-0397, Japan, New Product Research Laboratory II, Daiichi Pharmaceutical Company Ltd., 16-13 Kita-Kasai 1-Chome, Edogawa-ku, Tokyo 134-8630, Japan, Department of Neuropathology and Neuroscience, Graduate School of Pharmaceutical Science, The University of Tokyo, 7-3-1 Hongo, Bunkyo-ku, Tokyo 113-0033, Japan, and Medical Research Council Laboratory of Molecular Biology, Hills Road, Cambridge CB2 2QH, U.K.

Received January 12, 2006; Revised Manuscript Received March 17, 2006

ABSTRACT: α-Synuclein is the major component of the filamentous inclusions that constitute defining characteristics of Parkinson's disease and other α-synucleinopathies. Here we have tested 79 compounds belonging to 12 different chemical classes for their ability to inhibit the assembly of α-synuclein into filaments in vitro. Several polyphenols, phenothiazines, porphyrins, polyene macrolides, and Congo red and its derivatives, BSB and FSB, inhibited α-synuclein filament assembly with IC_{50} values in the low micromolar range. Many compounds that inhibited α-synuclein assembly were also found to inhibit the formation of Aβ and tau filaments. Biochemical analysis revealed the formation of soluble oligomeric α-synuclein in the presence of inhibitory compounds, suggesting that this may be the mechanism by which filament formation is inhibited. Unlike α-synuclein filaments and protofibrils, these soluble oligomeric species did not reduce the viability of SH-SY5Y cells. These findings suggest that the soluble oligomers formed in the presence of inhibitory compounds may not be toxic to nerve cells and that these compounds may therefore have therapeutic potential for α-synucleinopathies and other brain amyloidoses.

Filamentous inclusions made of the protein α-synuclein in nerve cells or glial cells are the defining neuropathological feature of a group of neurodegenerative diseases which include Parkinson's disease (PD),[1] dementia with Lewy bodies (DLB), and multiple-system atrophy (MSA) (*1*). In these so-called "α-synucleinopathies", α-synuclein is deposited in a hyperphosphorylated form (*2*−*8*). Missense mutations (A30P, E46K, and A53T) in the α-synuclein gene cause familial forms of PD and DLB (*9*−*11*). Furthermore, multiplications (duplication and triplication) of a region on the long arm of chromosome 4 that encompasses the α-synuclein gene cause an inherited form of PD dementia (*12*−*14*), indicating that the simple overproduction of wild-type α-synuclein is sufficient to cause PD dementia.

α-Synuclein is a 140-amino acid protein of unknown function that is abundantly expressed in brain, where it is concentrated in presynaptic nerve terminals (*15*, *16*). The amino-terminal region of α-synuclein (residues 7−87) consists of seven imperfect repeats, each 11 amino acids in length, with the consensus sequence KTKEGV. The repeats are continuous, except for a four-amino acid stretch between repeats 4 and 5, and partially overlap with a hydrophobic region (amino acids 61−95). The carboxy-terminal region (amino acids 96−140) is negatively charged. α-Synuclein is a natively unfolded protein with little ordered secondary structure that binds to lipid membranes through its amino-terminal repeats, indicating that it may be a physiological lipid-binding protein (*17*−*21*). Upon binding to lipid membranes, α-synuclein adopts structures rich in α-helical character (*18*, *20*−*25*).

Recombinant α-synuclein readily assembles into filaments that share many of the morphological and ultrastructural characteristics of the filaments present in human brain (*26*−*29*). Assembly is a nucleation-dependent process and occurs through sequences located in the 100 amino-terminal amino acids of α-synuclein (*30*, *31*). The carboxy-terminal region, in contrast, inhibits assembly (*26*, *29*, *32*). Although α-synuclein is largely unstructured, its negatively charged C-terminus makes long-range contacts with the central

† This work was supported by Grants-in-Aid for Scientific Research on Priority Areas (Research on Pathomechanisms of Brain Disorders) from the Ministry of Education, Culture, Sports, Science and Technology of Japan (to T.I., S.H., and M.H.).

* To whom correspondence should be addressed: Department of Molecular Neurobiology, Tokyo Institute of Psychiatry, 2-1-8 Kamikitazawa, Setagaya-ku, Tokyo 156-8585, Japan. Telephone: +81 3 3304 5701. Fax: +81 3 3329 8035. E-mail: masato@prit.go.jp.

‡ Tokyo Institute of Psychiatry.

§ Tokyo Metropolitan University.

∥ Daiichi Pharmaceutical Co. Ltd.

⊥ The University of Tokyo.

@ Medical Research Council Laboratory of Molecular Biology.

[1] Abbreviations: PD, Parkinson's disease; DLB, dementia with Lewy bodies; MSA, multiple-system atrophy; ThS, thioflavin S; HPLC, high-performance liquid chromatography; DMSO, dimethyl sulfoxide; PBS, phosphate-buffered saline; ThT, thioflavin T; DAPH, 4,5-dianilinophthalimide; BSB, 1-bromo-2,5-bis(3-carboxystyryl)benzene; FSB, 1-fluoro-2,5-bis(3-hydroxycarbonyl-4-hydroxystyryl)benzene; MTT, 3-(4,5-dimethylthiazol-2-yl)-2,5-diphenyltetrazolium bromide; PET, positron emission tomography; MRI, magnetic resonance imaging; FTDP-17, frontotemporal dementia and parkinsonism linked to chromosome 17.

10.1021/bi0600749 CCC: $33.50
Published on Web 04/21/2006

hydrophobic region (*33*, *34*). Perturbation of these interactions is likely to expose hydrophobic surfaces, facilitating filament formation.

Mutations E46K and A53T in α-synuclein have been found to accelerate the rate of filament assembly (*28*, *35*, *36*). The A30P mutation has been reported to increase the total rate of aggregation of α-synuclein (*37*−*39*) but to slow the rate of formation of mature filaments (*40*). X-ray fiber diffraction and electron diffraction analyses have shown that the transition from natively unfolded to cross-β structure underlies the assembly of α-synuclein into filaments (*29*). It is therefore appropriate to consider the α-synucleinopathies a form of brain amyloidosis.

The conversion of a small number of soluble peptides and proteins into insoluble filaments is believed to be the central event in the pathogenesis of the most common neurodegenerative diseases (*41*, *42*). Consequently, many current therapeutic strategies are aimed at inhibiting filament formation and at promoting filament clearance. They include the use of antibodies, synthetic peptides, molecular chaperones, and chemical compounds. Among these, small organic molecules have been extensively tested for their ability to inhibit filament formation in vitro, particularly in relation to Aβ deposition (*43*), the formation of protease-resistant forms of the prion protein (*44*), the aggregation of huntingtin (*45*), and, more recently, the heparin-induced formation of tau filaments (*46*, *47*). Less is known about small organic molecules that inhibit the formation of α-synuclein filaments. Several studies have described inhibition of filament formation by catecholamines (*48*−*50*), with other studies reporting inhibition by the polyphenol baicalein (*51*), the porphyrin phthalocyanine (*52*), and the anti-tuberculosis drug rifampicin (*53*).

Here we have investigated the effects of 79 compounds belonging to 12 different chemical classes on α-synuclein filament formation. The ability of these compounds to inhibit the assembly of Aβ and tau protein was investigated in parallel. Filament formation was assessed by electron microscopy, thioflavin S (ThS) fluorescence, and the formation of sarkosyl-insoluble α-synuclein. Compounds belonging to seven chemical classes (polyphenols, porphyrins, phenothiazines, polyene macrolides, rifamycins, Congo red and derivatives, and terpenoids) inhibited α-synuclein filament formation. By SDS−PAGE, inhibition of assembly was reflected in a large reduction in the level of sarkosyl-insoluble α-synuclein and the accumulation of soluble, SDS-resistant dimers and oligomers. Unlike α-synuclein filaments and protofibrils, these soluble species did not reduce the viability of human dopaminergic neuroblastoma SH-SY5Y cells.

EXPERIMENTAL PROCEDURES

Expression and Purification of α-Synuclein Proteins. Human α-synuclein(1−140) and α-synuclein(1−120) were expressed in *Escherichia coli* BL21(DE3) cells and purified using boiling, Q-Sepharose (for 1−140) or SP-Sepharose (for 1−120) ion exchange chromatography, and ammonium sulfate precipitation, as described previously (*54*). During the course of the analysis of dimeric α-synuclein, we noticed that a cysteine residue was incorporated at position 136 instead of a tyrosine in ~20% of bacterially expressed human α-synuclein and that mutagenesis of codon 136 (TAC to TAT) resulted in the expression of α-synuclein lacking cysteine (*55*). Therefore, the Y136-TAT construct was used in all experiments. α-Synuclein proteins were dialyzed against 30 mM Tris-HCl (pH 7.5) and cleared by centrifugation at 113000*g* for 20 min. Following separation by reverse phase high-performance liquid chromatography (HPLC) (Aquapore RP300 column), the absorbance at 215 nm was measured and compared with that of α-synuclein of known concentration, to give the concentration of the freshly purified proteins. For immunoblotting, aliquots of reaction mixtures were separated by SDS−PAGE, blotted onto a PVDF membrane, blocked with 3% gelatin/PBS, and incubated overnight at room temperature with antibody Syn102 (1:1000 dilution), which recognizes residues 131−140 of human α-synuclein, in a 10% fetal calf serum/PBS solution. Following washing, the blots were incubated for 2 h at room temperature with biotinylated secondary antibody (1:500) (Vector Laboratories). Following further washing, the blots were incubated with peroxidase-labeled avidin−biotin (Vector Laboratories) for 30 min at room temperature and developed with NiCl-enhanced diaminobenzidine (Sigma).

α-Synuclein Filament Assembly and Inhibitor Testing. The compounds listed in Table 1 were dissolved in dimethyl sulfoxide (DMSO) and kept as 20 mM stock solutions. Purified recombinant human α-synuclein(1−140) and α-synuclein(1−120) (2 mg/mL) were incubated with shaking (200 rpm) at 37 °C for 72 h in 50 μL of 30 mM Tris-HCl (pH 7.5) containing 0.02% sodium azide, in the presence or absence of 200 μM compound. For a quantitative assessment of filament formation, the amount of sarkosyl-insoluble α-synuclein and the level of ThS fluorescence were measured. Sarkosyl-soluble and sarkosyl-insoluble α-synuclein were prepared as follows. Aliquots (10 μL) of assembly mixtures were removed and added to 40 μL of 30 mM Tris-HCl (pH 7.5) containing 1% sarkosyl. This was followed by a 20 min centrifugation at 453000*g*. The supernatants (sarkosyl-soluble) were removed and the pellets (sarkosyl-insoluble) resuspended in 50 μL of sample buffer, followed by SDS−PAGE. Following staining with Coomassie Brilliant Blue, the intensities of the sarkosyl-insoluble α-synuclein bands were quantified by scanning densitometry, as described previously (*47*). The supernatants were stained with the silver stain MS kit (Wako). For ThS fluorescence, aliquots (10 μL) of the assembly mixtures were removed and brought to 300 μL with 5 μM ThS (Sigma-Aldrich) in 20 mM MOPS (pH 6.8). Fluorimetry was performed using a Hitachi F4000 fluorescence spectrophotometer (set at 440 nm for excitation and 521 nm for emission), as described previously (*47*). The results were expressed as the percentage of α-synuclein assembly in the absence of compound (taken to be 100%). Statistical analysis was carried out with an unpaired *t* test using Kai plot software, and the results were expressed as the means ± the standard deviation. IC_{50} values were calculated for each compound by quantifying the amounts of sarkosyl-insoluble α-synuclein. For a semiquantitative assessment of filament formation, electron microscopy was used. Aliquots of assembly mixtures were placed on collodion-coated 300-mesh copper grids, stained with 2% phosphotungstate, and micrographs were recorded at a nominal magnification of 10000× on a JEOL 1200EX electron microscope.

Table 1: Inhibitors of Aβ, α-Synuclein, and Tau Filament Formation

no.	compound	IC_{50} (μM) Aβ	α-synuclein	tau
polyphenols				
A1	apigenin	>40	>80	>200
A2	baicalein	4.5	8.2	2.7
A3	(+)-catechin	>40	>80	>200
A4	(-)-catechin gallate	5	21.4	>200
A5	chlorogenic acid	>40	>80	>200
A6	curcumin	1.7	>80	>200
A7	cyanidin	4	10.3	33.3
A8	daidzein	>40	>80	>200
A9	delphinidin	3	6.5	6.9
A10	2,2′-dihydroxybenzophenone	>40	>80	>200
A11	4,4′-dihydroxybenzophenone	>40	>80	>200
A12	dopamine chloride	28.6	7.1	>200
A13	(−)-epicatechin	>40	29.9	>200
A14	(−)-epicatechin 3-gallate	3	14.5	4.5
A15	epigallocatechin	7	10.6	8.4
A16	epigallocatechin gallate	2	9.8	9.6
A17	exifone	0.7	2.5	3.3
A18	(−)-gallocatechin	7	8.9	13.3
A19	(−)-gallocatechin gallate	1.5	3.6	1
A20	gingerol	25	>80	>200
A21	gossypetin	1.3	5.6	2
A22	hinokiflavone	5	8.1	>200
A23	hypericin	0.9	7.5	26.8
A24	kaempferol	8	>80	>200
A25	luteolin	3	28	>200
A26	myricetin	0.9	13.3	1.2
A27	naringenin	25	>80	>200
A28	2,3,4,2′,4′-pentahydroxybenzophenone	2.8	28.3	2.4
A29	procyanidin B1	14	7.3	27.5
A30	procyanidin B2	>40	4.3	>200
A31	purpurogallin	0.5	12.9	5.6
A32	quercetin	5	20	>200
A33	rosmarinic acid	12	4.8	16.6
A34	rutin	32	>80	>200
A35	(+)-taxifolin	>40	>80	>200
A36	2,2′,4,4′-tetrahydroxybenzophenone	>40	>80	>200
A37	theaflavine	2	5.8	7.9
A38	(+)-α-tocopherol	>40	10.9	107.7
A39	2,3,4-trihydroxybenzophenone	3.1	18.6	12.2
anthracycline				
B1	daunorubicin hydrochloride	1.4	>80	>200
benzothiazoles				
C1	2-(4-aminophenyl)-6-methyl-benzothiazole	2	>80	>200
C2	basic blue 41	1.4	>80	>200
C3	2-[4-(dimethylamino)phenyl]-6-methylbenzothiazole	2	>80	>200
C4	3,3′-dipropyl thiodicarbocyanine iodide (DTCI)	0.3	>80	>200
lignans				
D1	magnolol	>40	>80	>200
D2	sesamin	>40	>80	>200
phenothiazines				
E1	acetopromazine maleate salt	>40	>80	>200
E2	azure A	0.4	>80	2.6
E3	azure C	0.2	>80	1.9
E4	chlorpromazine hydrochloride	>40	>80	>200
E5	lacmoid	1.4	14.7	31.2
E6	methylene blue	2.3	>80	1.9
E7	perphenazine	>40	38.7	>200
E8	promazine hydrochloride	>40	>80	>200
E9	propionylpromazine hydrochloride	>40	>80	>200
E10	quinacrine	8.4	>80	79.6
E11	quinacrine mustard	1.2	>80	3.1
polyene macrolides				
F1	amphotericin B	2.2	27.1	>200
F2	filipin III	14.6	78.2	>200
porphyrins				
G1	ferric dehydroporphyrin IX	0.2	9.7	1.4
G2	hematin (from bovine blood)	0.2	15	10.4
G3	phthalocyanine tetrasulfonate	3.2	27.5	67
rifamycin				
H1	rifampicin	4.9	46.2	>200
steroids				
I1	taurochenodeoxycholic acid	>40	>80	>200
I2	taurohydroxycholic acid	>40	>80	>200
I3	taurolithocholic acid	>40	>80	>200
I4	taurolithocholic acid 3-sulfate	>40	>80	>200
I5	tauroursodeoxycholic acid	>40	>80	>200
Congo red and derivatives				
J1	Congo red	0.9	2.3	2.2
J2	chlorazol black E	0.3	16.4	>200
J3	BSB	6.4	4	18.2
J4	FSB	1.9	12.4	35.7
J5	Ponceau SS	1.2	>80	>200
terpenoids				
K1	asiatic acid	>40	45	>200
K2	ginkgolide A	>40	>80	>200
K3	ginkgolide B	11	>80	>200
K4	ginkgolide C	>40	>80	>200
others				
L1	4,5-dianilinophthalimide (DAPH)	2.9	>80	>200
L2	methyl yellow	1.5	>80	>200

Aβ and Tau Filament Assemblies and Inhibitor Testing. Monomeric Aβ(1−40) (1 mM, Peptide Institute Inc., Osaka, Japan) in distilled water was diluted with phosphate-buffered saline (PBS, pH 7.5) to a final concentration of 15 μM and incubated at 37 °C for 24 h in 40 μL of PBS, containing 5 μM thioflavin T (ThT), in the presence or absence of compounds (0.3−40 μM). Fluorimetry was performed using a Biolumin960 fluorescence spectrophotometer (set at 450 nm for excitation and 485 nm for emission, Amersham Biosciences) (*56*), and IC_{50} values were calculated. For the analysis of oligomeric Aβ, Aβ(1−40) was incubated at 37 °C for 4 days in 40 μL of PBS at a concentration of 75 μM in the presence or absence of 200 μM compound. Aliquots (10 μL) of mixtures were removed and added to 40 μL of 30 mM Tris-HCl (pH 7.5) containing 1% sarkosyl and the mixtures centrifuged at 25 °C for 20 min at 453000*g*. The supernatants (sarkosyl-soluble) were removed and the pellets (sarkosyl-insoluble) resuspended in 50 μL of sample buffer, run on a SDS−PAGE gel, and visualized by silver staining. The 412-amino acid isoform of human brain tau (*57*) was expressed from cDNA clone htau46 and purified, as described previously (*47*, *58*). The effect of inhibitory compounds on the heparin-induced filament formation of tau was measured by quantifying the levels of Sarkosyl-insoluble tau (*47*).

Preparation of α-Synuclein Filaments, Protofibrils, and Soluble Oligomers. α-Synuclein filaments were obtained by pelleting the assembly mixtures at 113000*g* for 20 min. Protofibrils were prepared as described previously (*59*). Briefly, purified α-synuclein was dialyzed against 20 mM NH_4HCO_3, lyophilized, and resuspended in PBS at 20 mg/mL. Following a 5 min centrifugation at 20000*g*, the supernatants were loaded onto a Superdex 200 gel filtration column (1 cm × 30 cm), eluted in 10 mM Tris-HCl (pH

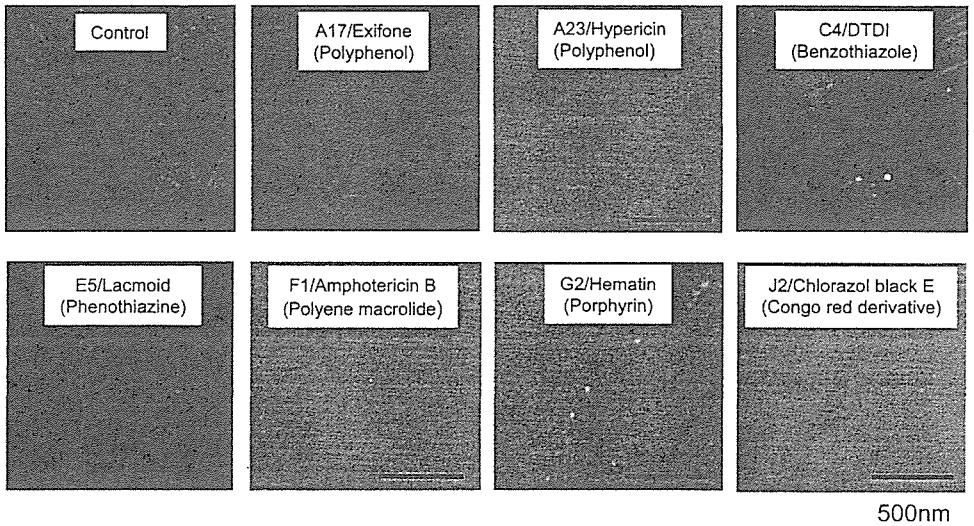

FIGURE 1: Semiquantitative assessment by electron microscopy of α-synuclein filament formation in the absence (Control) or presence of compounds. Small numbers of filaments or no filaments were seen in the presence of exifone (A17), hypericin (A23), lacmoid (E5), amphotericin B (F1), hematin (G2), and chlorazol black E (J2). Filament numbers similar to controls were observed in the presence of 3,3′-dipropylthiocarbocyanine iodide (DTCI) (C4). A typical experiment is shown. Similar results were obtained in three separate experiments.

7.5) containing 150 mM NaCl, and monitored at 215 nm. The material eluting in the void volume was defined as protofibrils. To prepare soluble oligomers, purified α-synuclein (9 mg/mL) was incubated with 2 mM inhibitory compound for 30 days at 37 °C in 30 mM Tris-HCl containing 0.1% sodium azide. The samples were then centrifuged for 20 min at 113000*g* and the supernatants run on a Sephadex G-25 column, to separate oligomers from unbound inhibitor (*52*). The eluates were then fractionated on a Superdex 200 gel filtration column, as described above. Protein concentrations were determined using HPLC and the BCA protein assay kit (Pierce).

Cytotoxicity Assay. A solution (100 μL) containing 10 000 SH-SY5Y cells in DMEM-F12 with 10% fetal calf serum was added to each well of a 96-well microtiter plate and left for 24 h in a humidified incubator at 37 °C and 5% CO_2. The medium was then replaced with 100 μL of serum-free medium, followed by the addition of the monomeric, soluble oligomeric, protofibrillar, and filamentous α-synuclein. Following a 6 h incubation, the cytotoxic effect of α-synuclein was assessed by measuring cellular redox activity with 3-(4,5-dimethylthiazol-2-yl)-2,5-diphenyltetrazolium bromide (MTT), following the manufacturer's (Sigma) instructions.

RESULTS

Inhibition of α-Synuclein Filament Assembly. Seventy-nine compounds belonging to 12 different chemical classes (listed in Table 1; see the Supporting Information for chemical structures) were tested for their ability to inhibit the assembly of full-length human α-synuclein into filaments, which was assessed by electron microscopy (Figure 1), thioflavin S fluorescence, and sarkosyl insolubility (Figure 2). By SDS−PAGE, a large reduction in the level of sarkosyl-insoluble α-synuclein and a corresponding increase in the level of sarkosyl-soluble protein were observed in the presence of several polyphenols (A17, A21, A26, and A31), phenothiazine E5, polyene macrolide F2, porphyrin G2, and Congo red derivative J2 (Figure 3). In the presence of inhibitors, dimeric and oligomeric, SDS-stable α-synuclein appeared in the sarkosyl-soluble fraction (Figure 3). Anthracyclines, benzothiazoles, lignans, steroids, 4,5-dianilinophthalimide (DAPH), and methyl yellow failed to inhibit α-synuclein filament formation, and SDS-stable oligomers were not observed. A representative example of each class of compound is shown in Figure 3.

Filament formation was quantified by measuring the levels of sarkosyl-insoluble α-synuclein and ThS fluorescence in the presence of each compound. In general, a good correlation was observed between the amounts of ThS fluorescence and sarkosyl-insoluble α-synuclein. However, for some benzothiazoles (C2 and C4), phenothiazines (E2, E3, and E6), porphyrin G3, and Congo red derivative J5, a large reduction in ThS fluorescence was observed, with only a slight change in the levels of sarkosyl-insoluble α-synuclein (Figure 2). The results observed by electron microscopy were in complete agreement with those from the sarkosyl experiments (Figure 1).

The IC_{50} values of all 79 compounds for inhibiting α-synuclein filament assembly were determined by quantifying the levels of sarkosyl-insoluble α-synuclein (Table 1). The effects of the same compounds on the assembly of Aβ and tau were assessed in parallel. For all three proteins, the inhibition of filament formation was concentration-dependent (data not shown). Strong inhibition of α-synuclein filament assembly (IC_{50} values of <10 μM) was observed with the polyphenol compounds baicalein (A2), delphinidin (A9), dopamine chloride (A12), epigallocatechin gallate (A16), exifone (A17), (−)-gallocatechin (A18), (−)-gallocatechin gallate (A19), gossypetin (A21), hinokiflavone (A22), hypericin (A23), procyanidin B1 (A29), procyanidin B2 (A30), rosmarinic acid (A33) and theaflavine (A37), the porphyrin ferric dehydroporphyrin IX (G1), Congo red (J1), and its derivative 1-bromo-2,5-bis(3-carboxystyryl)benzene (BSB) (J3). Vitamin E (α-tocopherol, A38) also exhibited a strong inhibitory effect, with an IC_{50} value of 10.9 μM. Other polyphenols (A4, A7, A13−A15, A25, A26, A28, A31, A32, A38, and A39), phenothiazines (E5 and E7), a polyene macrolide (F1), porphyrins (G2 and G3), and Congo red derivatives (J2 and J4) inhibited the assembly of α-synuclein

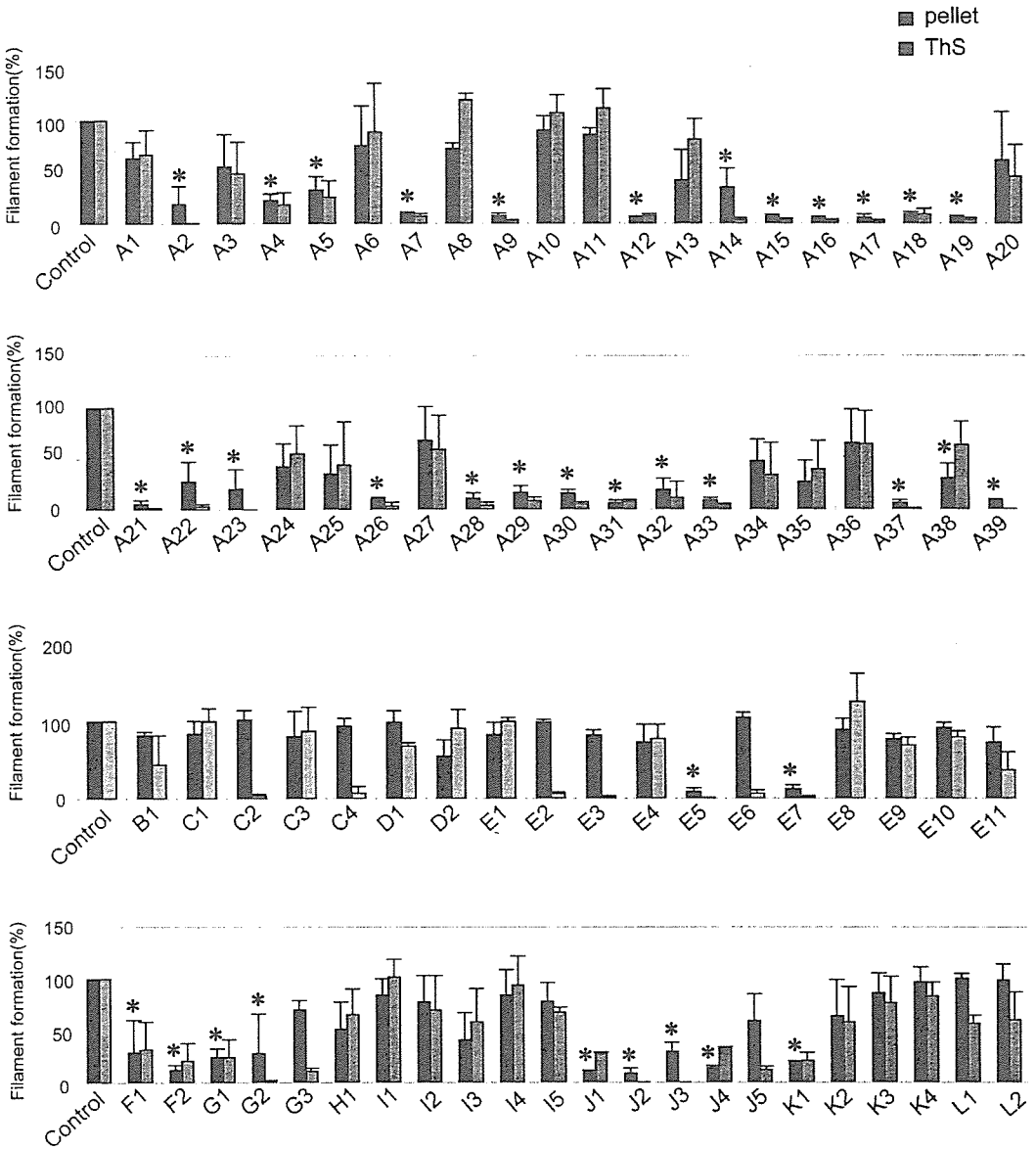

FIGURE 2: Quantitation of α-synuclein filament formation in the absence (Control) or presence of compounds using ThS fluorescence and sarkosyl insolubility. A significant reduction in the amount of sarkosyl-insoluble α-synuclein (black bars) and ThS fluorescence (gray bars) was observed in the presence of polyphenols (A2, A4, A5, A7, A9, A12, A14−A19, A21−A23, A26, A28−A33, A37, and A39), phenothiazines (E5 and E7), polyene macrolides (F1 and F2), porphyrins (G1 and G2), Congo red and its derivatives (J1−J4), and terpenoid K1. The results are expressed as means ± the standard error ($n = 3$; asterisks denote $p < 0.001$). With some compounds (C2, C4, E2, E3, E6, G3, and J5), ThS fluorescence was reduced, but the amount of sarkosyl-insoluble α-synuclein was not changed relative to controls.

less strongly (IC_{50} values of 10−40 μM). Rifampicin (H1) was weakly inhibitory (IC_{50} value of 46 μM).

The role of the carboxy-terminal region of α-synuclein was investigated by incubating α-synuclein(1−120) with the following at 200 μM: polyphenols dopamine chloride (A12) and exifone (A17), the phenothiazine lacmoid (E5), the porphyrin hematin (G2), and the Congo red derivative chlorazol black E (J2). All five compounds strongly inhibited the assembly of full-length α-synuclein; however, unlike exifone and lacmoid, dopamine chloride, hematin, and chlorazol black E did not inhibit filament formation of α-synuclein(1−120) (see the Supporting Information).

Inhibition of Aβ Fibril Formation. We investigated whether inhibition of Aβ fibril formation is accompanied by the formation of SDS-stable dimers and oligomers. As shown in Figure 4, both in the absence of compounds and in the presence of noninhibitory compounds, soluble dimer and oligomer levels were very low. In the presence of compounds that inhibit Aβ and α-synuclein assembly, such as some polyphenols (A17, A21, A26, and A33), the phenothiazine lacmoid (E5), and the porphyrin hematin (G2), a strong dimer band and more variable oligomer bands were observed in the sarkosyl-soluble fraction (Figure 4).

Cytotoxicity Studies. Protofibrils and soluble oligomeric species of α-synuclein were prepared by gel filtration chromatography (Figures 5 and 6). Protofibrils were defined as the material eluting in the void volume (fraction 1) of the column, as proposed previously (*59*). SH-SY5Y cells were exposed for 6 h to monomeric, soluble oligomeric, protofibrillar, or filamentous human α-synuclein. Cell viability was evaluated using reduction of MTT to MTT formazan and compared with that of vehicle-treated cells. In cells exposed to monomeric α-synuclein, there was no significant reduction in cell viability. This stood in marked contrast to

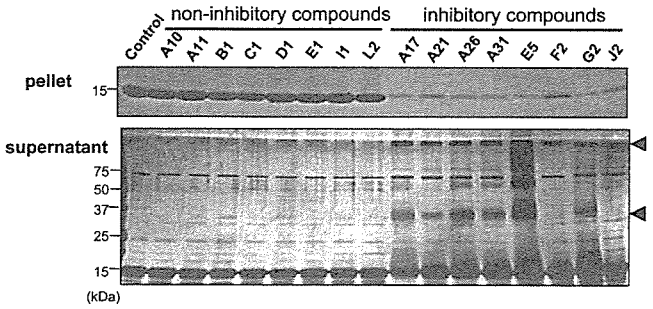

FIGURE 3: Formation of soluble α-synuclein oligomers in the presence of inhibitory compounds. Sarkosyl-insoluble (pellet, top panel) and sarkosyl-soluble (supernatant, bottom panel) α-synuclein was prepared following incubation of α-synuclein in the absence (Control) or presence of compounds (A10, A11, A17, A21, A26, A31, B1, C1, D1, E1, E5, F2, G2, I1, J2, and L2). Via SDS–PAGE, SDS-stable, high-molecular weight α-synuclein (arrowheads) was detected in the supernatants of samples incubated with inhibitory compounds, but not in the supernatants of controls or samples incubated with noninhibitory compounds. The presence of high-molecular weight α-synuclein in the supernatant was accompanied by a reduction in the levels of monomeric α-synuclein in the pellet. A typical experiment is shown. Similar results were obtained in three separate experiments.

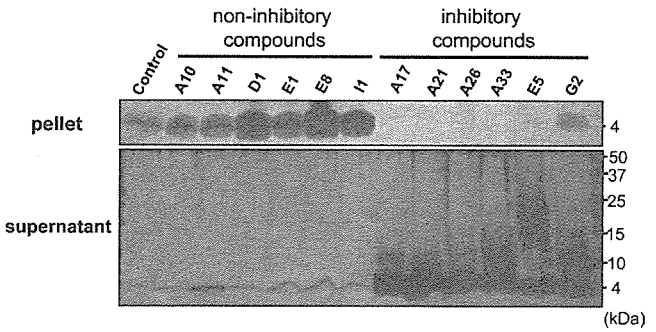

FIGURE 4: Formation of soluble Aβ oligomers in the presence of inhibitory compounds. Sarkosyl-insoluble (pellet, top panel) and sarkosyl-soluble (supernatant, bottom panel) Aβ was prepared following incubation of Aβ in the absence (Control) or presence of compounds (A10, A11, A17, A21, A26, A33, D1, E1, E5, E8, G2, and I1). Via SDS–PAGE, SDS-stable, soluble oligomeric Aβ was detected in the presence of inhibitory compounds, but not in the presence of noninhibitory compounds. A typical experiment is shown. Similar results were obtained in three separate experiments.

α-synuclein filaments, which were cytotoxic. When they were used at 500 nM, approximately 60% of cells were killed, with ~50% cell death at 50 nM filaments (Figure 5). Protofibrils were also cytotoxic, with 30% cell death at 500 nM and 10% cell loss at 50 nM. The toxicities of filaments and protofibrils were concentration-dependent (Figure 5). Next, we tested the cytotoxicity of soluble oligomeric species obtained following incubation of α-synuclein in the presence of inhibitory compounds dopamine chloride (A12), exifone (A17), lacmoid (E5), and hematin (G2). In presence of each inhibitory compound, five protein peaks were resolved by gel filtration (Figure 6) and tested individually in the cytotoxicity assay. In contrast to filaments and protofibrils, none of the soluble oligomeric fractions of α-synuclein that were tested exhibited cytotoxicity in this assay (Figure 6).

DISCUSSION

Thioflavin S fluorescence, levels of sarkosyl-insoluble α-synuclein, and electron microscopic examination were used

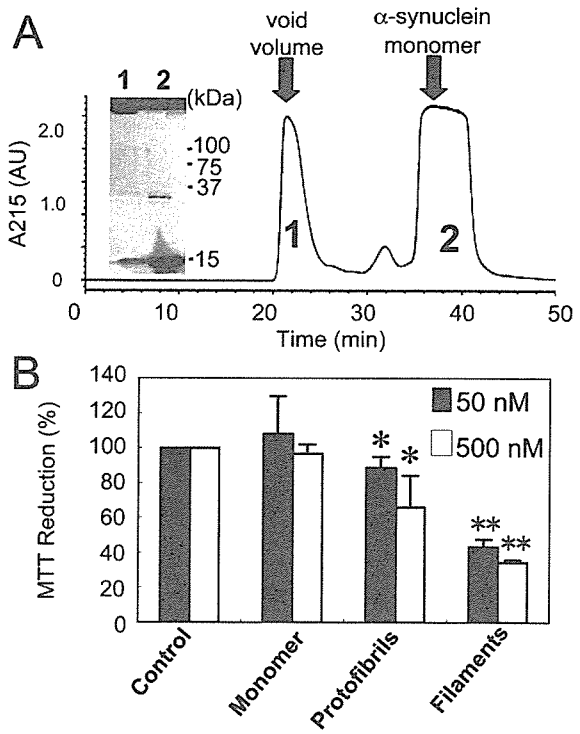

FIGURE 5: Cytotoxicity of α-synuclein monomer, protofibrils, and filaments. α-Synuclein protofibrils and soluble monomer were fractionated by gel filtration chromatography and analyzed by Western blotting (WB) using antibody syn102. The cytotoxicity of α-synuclein monomers, protofibrils, and filaments at 50 nM (black bars) or 500 nM (white bars) was assessed using the MTT assay. Protofibrils and filaments exhibited dose-dependent cytotoxicity. The results are presented as percent MTT reduction, with the values obtained in the absence of added α-synuclein taken as 100%. They are expressed as means ± the standard error ($n = 6$; one asterisk denotes $p < 0.01$, and two asterisks denote $p < 0.001$).

to investigate the effects of 79 compounds belonging to 12 chemical classes on the assembly of α-synuclein into filaments. Compounds belonging to seven classes (polyphenols, phenothiazines, polyene macrolides, porphyrins, rifamycins, Congo red and its derivatives, and terpenoids) inhibited filament assembly. The three methods used for monitoring filament assembly gave similar results in the presence of inhibitors, except for thioflavin S (a benzothiazole), which could not be used for testing inhibition by some benzothiazoles and phenothiazines. It could also not be used in the presence of Congo red and its derivatives.

A number of polyphenols [baicalein, delphinidin, dopamine chloride, epigallocatechin gallate, exifone, (−)-gallocatechins, gossypetin, hinokiflavone, hypericin, procyanidins, rosmarinic acid, and theaflavine], the porphyrin compound ferric dehydroporphyrin IX, and Congo red and its derivative BSB inhibited α-synuclein filament assembly with IC_{50} values of <10 μM. Other polyphenols [cyanidin, (−)-epicatechin 3-gallate, epigallocatechin, myricetin, purpurogallin, (+)-α-tocopherol, and 2,3,4-trihydroxybenzophenone], as well as the phenothiazine lacmoid, the porphyrin hematin, and the Congo red derivatives chlorazol black E and 1-fluoro-2,5-bis(3-hydroxycarbonyl-4-hydroxystyryl)benzene (FSB), inhibited filament formation with IC_{50} values of 10−20 μM. The phenothiazine perphenazine, the polyene macrolides amphotericin B and filipin III, the terpenoid asiatic acid, and rifampicin were less potent. Anthracyclines, benzothiazoles, lignans, steroids, DAPH, and methyl yellow were without

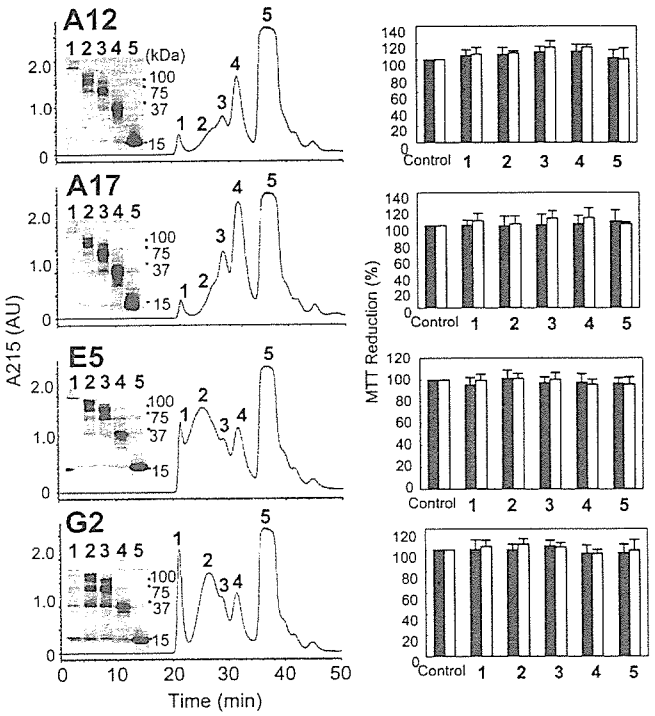

FIGURE 6: Soluble α-synuclein oligomers formed in the presence of inhibitory compounds do not reduce the viability of SH-SY5Y cells. α-Synuclein soluble oligomers were fractionated by gel filtration chromatography and analyzed by WB using antibody syn102. In the presence of inhibitory compounds A12, A17, E5, and G2, SDS-resistant dimers (fraction 4) and oligomers (fractions 1−3) formed. Fraction 5 corresponds to the α-synuclein monomer. In the absence of inhibitory compounds, oligomers did not form (not shown). The cytotoxicity of soluble oligomers was assessed using the MTT assay. In contrast to protofibrils and filaments, monomeric α-synuclein and fractions 1−5 of oligomeric α-synuclein at 50 nM (black bars) or 500 nM (white bars) were not cytotoxic. The results are presented as the percent MTT reduction, with the values obtained in the absence of added α-synuclein taken as 100%. They are expressed as means ± the standard error (n = 6).

effect (IC_{50} values of >80 μM). These findings establish that polyphenols constitute a major class of compounds that can inhibit the assembly of α-synuclein. Many polyphenols are natural substances present in beverages obtained from plants, fruits, and vegetables. Besides inhibiting the aggregation of α-synuclein, Aβ, and tau, they are also known to have neuroprotective effects in a number of paradigms (*60*). Of the 39 compounds that were tested, 26 inhibited α-synuclein assembly, 29 inhibited Aβ assembly, and 19 inhibited tau filament formation. In particular, some catechins and vitamin E (α-tocopherol) were inhibitory. We confirmed and extended recent work showing inhibition of α-synuclein filament formation by baicalein, dopamine, and a number of catecholamines. Previous work suggested that two adjacent phenolic OH groups may be required for the inhibition of α-synuclein filament formation via covalent modification (*48*−*51*). Of the 27 inhibitory polyphenols identified here, 23 had two adjacent phenolic OH groups. Furthermore, all polyphenols with three OH groups in the ring (a total of 15 compounds) were inhibitory (Supporting Information), suggesting that adjacent phenolic OH groups may indeed play an important role. However, some compounds (hinokiflavone, hypericin, and α-tocopherol) lacking adjacent phenolic OH groups were also inhibitory. Additional studies are needed to better understand these structure−activity relationships.

Porphyrins have previously been shown to inhibit the assembly of Aβ and tau (*47*). Prior to the work presented here, phthalocyanine tetrasulfonate was the only porphyrin known to inhibit α-synuclein filament assembly (*52*). We found a weak inhibitory effect of phthalocyanine tetrasulfonate, with stronger inhibition by the porphyrins ferric dehydroporphyrin IX and hematin. In contrast to a previous report (*52*), we failed to detect disassembly of α-synuclein filaments in the presence of phthalocyanine tetrasulfonate. Consistent with previous work (*53*), rifampicin inhibited α-synuclein assembly, albeit not very potently. Prior to the study presented here, inhibition of α-synuclein filament formation by phenothiazines had not been reported. Of the 11 compounds that were tested, lacmoid and perphenazine were inhibitory. As shown previously (*47*), compounds lacking a side chain at position 9 of the phenothiazine ring were inhibitory toward the assembly of Aβ and tau. However, this was not true of α-synuclein aggregation, suggesting a difference in conformation between oligomers and filaments of α-synuclein and those of Aβ and tau. Congo red was strongly inhibitory toward the assembly of α-synuclein and tau. The same was true of Aβ fibril formation, confirming previous results (*61*, *62*). Moreover, Congo red has also been shown to prevent the aggregation and infectivity of the prion protein (*63*, *64*) and the aggregation of huntingtin (*65*, *66*). Congo red derivatives BSB and FSB also inhibited the assembly of Aβ, α-synuclein, and tau. Unlike Congo red, they cross the blood−brain barrier and are currently being developed as reagents for visualizing Aβ deposits in vivo by positron emission tomography (PET) and magnetic resonance imaging (MRI) (*67*−*69*). BSB has also been shown to label some α-synuclein deposits in brain sections from cases of MSA and DLB and some tau deposits in cases of Alzheimer's disease, progressive supranuclear palsy, and frontotemporal dementia and parkinsonism linked to chromosome 17 (FTDP-17) (*70*). Overall, a number of compounds inhibited the assembly of Aβ, α-synuclein, and tau, in line with findings suggesting that soluble amyloid oligomers can have structural features in common (*71*). Almost all the compounds that inhibited α-synuclein assembly also inhibited Aβ assembly. Exceptions were (−)-epicatechin, procyanidin B2, α-tocopherol, perphenazine, and asiatic acid. Conversely, several compounds inhibited Aβ assembly without interfering with α-synuclein and tau filament formation. They included all the benzothiazoles that were tested, several polyphenols (curcumin, gingerol, kaempferol, naringenin, and rutin), the anthracycline daunorubicin hydrochloride, the Congo red derivative Ponceau S, the terpenoid ginkgolide B, and DAPH and methyl yellow.

Previous work has shown that the C-terminal region of α-synuclein is a negative regulator of filament assembly (*26*, *29*, *32*), probably through long-range interactions with part of the hydrophobic region (*33*, *34*). We therefore investigated the ability of dopamine chloride, exifone, lacmoid, hematin, and chlorazol black E to inhibit the assembly of α-synuclein (1−120). In contrast to that of full-length α-synuclein, the assembly of α-synuclein(1−120) was not inhibited by dopamine chloride, hematin, or chlorazol black E. Exifone and lacmoid inhibited but did not abolish filament formation of α-synuclein(1−120). These findings establish an important

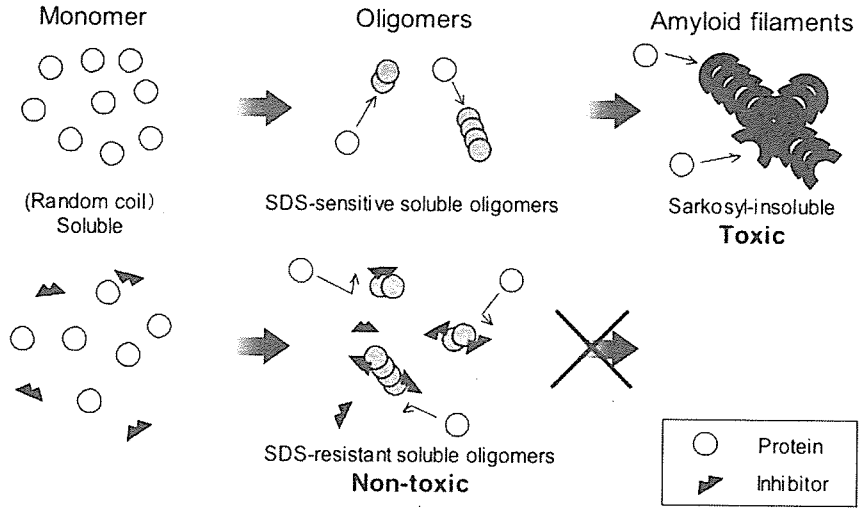

FIGURE 7: Model for the inhibition of amyloid filament formation by small compounds.

role for the C-terminal region of α-synuclein in the inhibition of filament assembly and suggest that the compounds used may bind to this region. They are in line with a recent study reporting that dopaminochrome inhibited assembly by binding to residues 125−129 of α-synuclein (*49*). Consistent with this report, we also found that covalent modification of α-synuclein was not required to prevent filament formation (not shown). Furthermore, binding of single-chain antibodies to the C-terminal region of α-synuclein has been shown to inhibit filament assembly (*72*). It remains to be determined whether the binding of inhibitory compounds and antibodies influences the long-range interactions between the C-terminus of α-synuclein and the hydrophobic region.

Analysis of the sarkosyl-soluble fraction of α-synuclein assemblies by SDS−PAGE revealed the presence of dimeric and oligomeric protein in the presence of inhibitory compounds. This was in marked contrast to the sarkosyl-insoluble, SDS-sensitive α-synuclein which formed in the absence of inhibitors. Dimers and oligomers were also observed upon incubation of Aβ with inhibitory compounds. These findings are reminiscent of what was observed when heparin-induced filament formation of tau protein was inhibited by some of the same compounds (*47*). It suggests that the compounds investigated here may inhibit filament formation of α-synuclein by stabilizing soluble, prefibrillar intermediates (Figure 7). The latter, whose precise mechanism of formation remains to be determined, may be intermediates in the pathway leading from monomeric to filamentous α-synuclein. A recent study (*73*) has shown that heat shock protein Hsp70 inhibits α-synuclein filament formation by binding to soluble prefibrillar intermediates, suggesting that small organic molecules and chaperone proteins may inhibit assembly of α-synuclein through similar mechanisms. Since soluble amyloid oligomers of Aβ, α-synuclein, and tau appear to have structural features in common (*71*), a number of compounds that inhibited the assembly of Aβ, α-synuclein, and tau may recognize and interact with this common structure. Other compounds only inhibited Aβ aggregation, indicating that they may recognize a conformation specific to Aβ.

The cytotoxicity of soluble oligomers was investigated in SH-SY5Y cells and compared with that of monomeric α-synuclein, protofibrils, and filaments. Monomers and soluble oligomers did not reduce cell viability. By contrast, protofibrils and filaments were markedly cytotoxic. These results indicate that the compounds investigated here inhibited not only filament formation but also the toxicity of α-synuclein. They demonstrate a link between filament formation and toxicity in this system, in agreement with earlier findings (*74*). Future experiments will investigate whether the same inhibitors have similar effects in model systems where α-synuclein filaments are present intracellularly rather than being added from the outside. Currently, it is not clear which α-synuclein species are the most detrimental to nerve cells and glial cells in Lewy body diseases and MSA, and in animal models thereof (*75*−*77*). This notwithstanding, these findings indicate that the soluble oligomeric species formed in the presence of inhibitory compounds may not be toxic to nerve cells and may hence have therapeutic potential.

ACKNOWLEDGMENT

We thank M. Mikami for assistance with the SDS−PAGE analysis and Drs. A. L. Fink (University of California) and F. Kametani (Tokyo Institute of Psychiatry) for helpful discussions.

SUPPORTING INFORMATION AVAILABLE

List of compounds tested and quantitation of α-synuclein (1−120) filament formation in the absence or presence of inhibitory compounds using sarkosyl insolubility. This material is available free of charge via the Internet at http://pubs.acs.org.

REFERENCES

1. Goedert, M. (2001) α-Synuclein and neurodegenerative diseases, *Nat. Rev. Neurosci. 2*, 492−501.
2. Spillantini, M. G., Schmidt, M. L., Lee, V. M.-Y., Trojanowski, J. Q., Jakes, R., and Goedert, M. (1997) α-Synuclein in Lewy bodies, *Nature 388*, 839−840.
3. Baba, M., Nakajo, S., Tu, P.-H., Tomita, T., Nakaya, K., Lee, V. M.-Y., Trojanowski, J. Q., and Iwatsubo, T. (1998) Aggregation of α-synuclein in Lewy bodies of sporadic Parkinson's disease and dementia with Lewy bodies, *Am. J. Pathol. 152*, 879−884.
4. Spillantini, M. G., Crowther, R. A., Jakes, R., Hasegawa, M., and Goedert, M. (1998) α-Synuclein in filamentous inclusions of Lewy

bodies from Parkinson's disease and dementia with lewy bodies, *Proc. Natl. Acad. Sci. U.S.A. 95*, 6469−6473.
5. Wakabayashi, K., Yoshimoto, M., Tsuji, S., and Takahashi, H. (1998) α-Synuclein immunoreactivity in glial cytoplasmic inclusions in multiple system atrophy, *Neurosci. Lett. 249*, 180−182.
6. Spillantini, M. G., Crowther, R. A., Jakes, R., Cairns, N. J., Lantos, P. L., and Goedert, M. (1998) Filamentous α-synuclein inclusions link multiple system atrophy with Parkinson's disease and dementia with Lewy bodies, *Neurosci. Lett. 251*, 205−208.
7. Tu, P. H., Galvin, J. E., Baba, M., Giasson, B., Tomita, T., Leight, S., Nakajo, S., Iwatsubo, T., and Trojanowski, J. Q. (1988) Glial cytoplasmic inclusions in white matter oligodendrocytes of multiple system atrophy brains contain insoluble α-synuclein, *Ann. Neurol. 44*, 415−422.
8. Fujiwara, H., Hasegawa, M., Dohmae, N., Kawashima, A., Masliah, E., Goldberg, M. S., Shen, J., Takio, K., and Iwatsubo, T. (2002) α-Synuclein is phosphorylated in synucleinopathy lesions, *Nat. Cell Biol. 4*, 160−164.
9. Polymeropoulos, M. H., Lavedan, C., Leroy, E., Ide, S. E., Dehejia, A., Dutra, A., Pike, B., Root, H., Rubenstein, J., Boyer, R., Stenroos, E. S., Chandrasekharappa, S., Athanassiadou, A., Papapetropoulos, T., Johnson, W. G., Lazzarini, A. M., Duvoisin, R. C., Di Iorio, G., Golbe, L. I., and Nussbaum, R. L. (1997) Mutation in the α-synuclein gene identified in families with Parkinson's disease, *Science 276*, 2045−2047.
10. Krüger, R., Kuhn, W., Müller, T., Woitalla, D., Graeber, M., Kösel, S., Przuntek, H., Epplen, J. T., Schöls, L., and Riess, O. (1998) Ala30Pro mutation in the gene encoding α-synuclein in Parkinson's disease, *Nat. Genet. 18*, 106−108.
11. Zarranz, J. J., Alegre, J., Gómez-Esteban, J. C., Lezcano, E., Ros, R., Ampuero, I., Vidal, L., Hoenicka, J., Rodriguez, O., Atarés, B., Llorens, V., Gomez Tortosa, E., del Ser, T., Munoz, D. G., and de Yebenes, J. G. (2004) The new mutation, E46K, of α-synuclein causes Parkinson and Lewy body dementia, *Ann. Neurol. 55*, 164−173.
12. Singleton, A. B., Farrer, M., Johnson, J., Singleton, A., Hague, S., Kachergus, J., Hulihan, M., Peuralinna, T., Dutra, A., Nussbaum, R., Lincoln, S., Crawley, A., Hanson, M., Maraganore, D., Adler, C., Cookson, M. R., Muenter, M., Baptista, M., Miller, D., Blancato, J., Hardy, J., and Gwinn-Hardy, K. (2003) α-Synuclein locus triplication causes Parkinson's disease, *Science 302*, 841.
13. Chartier-Harlin, M. C., Kachergus, J., Roumier, C., Mouroux, V., Douay, X., Lincoln, S., Levecque, C., Lavor, L., Andrieux, J., Hulihan, M., Waucquier, N., Defebre, L., Amouyel, P., Farreer, M., and Destée, A. (2004) α-Synuclein locus duplication as a cause of familial Parkinson's disease, *Lancet 364*, 1167−1169.
14. Ibanez, P., Bonnet, A.-M., Débarges, B., Lohmann, E., Tison, F., Pollak, P., Agid, Y., Dürr, A., and Brice, A. (2004) Causal relation between α-synuclein gene duplication and familial Parkinson's disease, *Lancet 364*, 1169−1171.
15. Ueda, K., Fukushima, H., Masliah, E., Xia, Y., Iwai, A., Yoshimoto, M., Otero, D. A., Kondo, J., Ihara, Y., and Saitoh, T. (1993) Molecular cloning of cDNA encoding an unrecognized component of amyloid in Alzheimer disease, *Proc. Natl. Acad. Sci. U.S.A. 90*, 11282−11286.
16. Jakes, R., Spillantini, M. G., and Goedert, M. (1994) Identification of two distinct synucleins from human brain, *FEBS Lett. 345*, 27−32.
17. Weinreb, P. H., Zhen, W., Poon, A. W., Conway, K. A., and Lansbury, P. T. (1996) NACP, a protein implicated in Alzheimer's disease and learning, is natively unfolded, *Biochemistry 35*, 13709−13715.
18. Davidson, W. S., Jonas, A., Clayton, D. F., and George, J. M. (1998) Stabilization of α-synuclein secondary structure upon binding to synthetic membranes, *J. Biol. Chem. 273*, 9443−9449.
19. Jensen, P. H., Nielsen, M. H., Jakes, R., Dotti, C. G., and Goedert, M. (1998) Binding of α-synuclein to brain vesicles is abolished by familial Parkinson's disease mutation, *J. Biol. Chem. 273*, 26292−26294.
20. Jo, E., McLaurin, J. A., Yip, C. M., St George-Hyslop, P., and Fraser, P. E. (2000) α-Synuclein membrane interactions and lipid specificity, *J. Biol. Chem. 275*, 34328−34334.
21. Perrin, R. J., Woods, W. S., Clayton, D. F., and George, J. M. (2000) Interaction of human α-synuclein and Parkinson's disease variants with phospholipids. Structural analysis using site-directed mutagenesis, *J. Biol. Chem. 275*, 34393−34398.
22. Eliezer, D., Kutluay, E., Bussell, R., and Browne, G. (2001) Conformational properties of α-synuclein in its free and lipid-associated states, *J. Mol. Biol. 307*, 1061−1073.
23. Chandra, S., Chen, X., Rizo, J., Jahn, R., and Südhof, T. (2003) A broken α-helix in folded α-synuclein, *J. Biol. Chem. 278*, 15313−15318.
24. Jao, C. C., Der-Sarkissian, A., Chen, J., and Langen, R. (2004) Structure of membrane-bound α-synuclein studied by site-directed spin labeling, *Proc. Natl. Acad. Sci. U.S.A. 101*, 8331−8336.
25. Ulmer, T. S., Bax, A., Cole, N. B., and Nussbaum, R. L. (2005) Structure and dynamics of micelle-bound human α-synuclein, *J. Biol. Chem. 280*, 9595−9603.
26. Crowther, R. A., Jakes, R., Spillantini, M. G., and Goedert, M. (1998) Synthetic filaments assembled from C-terminally truncated α-synuclein, *FEBS Lett. 436*, 309−312.
27. El-Agnaf, O. M. A., Jakes, R., Curran, M. D., and Wallace, A. (1998) Effects of the mutations Ala30 to Pro and Ala53 to Thr on the physical and morphological properties of α-synuclein protein implicated in Parkinson's disease, *FEBS Lett. 440*, 67−70.
28. Conway, K. A., Harper, J. D., and Lansbury, P. T. (1998) Accelerated *in vitro* fibril formation by a mutant α-synuclein linked to early-onset Parkinson disease, *Nat. Med. 4*, 1318−1320.
29. Serpell, L. C., Berriman, J., Jakes, R., Goedert, M., and Crowther, R. A. (2000) Fiber diffraction of synthetic α-synuclein filaments shows amyloid-like cross-β conformation, *Proc. Natl. Acad. Sci. U.S.A. 97*, 4897−4902.
30. Miake, H., Mizusawa, H., Iwatsubo, T., and Hasegawa, M. (2002) Biochemical characterization of the core structure of α-synuclein filaments, *J. Biol. Chem. 277*, 19213−19219.
31. Der-Sarkissian, A., Jao, C. J., Chen, J., and Langen, R. (2003) Structural organization of α-synuclein fibrils studied by site-directed spin labeling, *J. Biol. Chem. 278*, 37530−37535.
32. Murray, I. V., Giasson, B. I., Quinn, S. M., Koppaka, V., Axelsen, P. H., Ischiropoulos, H., Trojanowski, J. Q., and Lee, V. M.-Y. (2003) Role of α-synuclein carboxy-terminus on fibril formation *in vitro*, *Biochemistry 42*, 8530−8540.
33. Dedmon, M. K., Lindorff-Larsen, K., Christodoulou, J., Vendruscolo, M., and Dobson, C. M. (2005) Mapping long-range interactions in α-synuclein using spin-label NMR and ensemble molecular dynamics simulations, *J. Am. Chem. Soc. 127*, 476−477.
34. Bertoncini, C. W., Jung, Y.-S., Fernandez, C. O., Hoyer, W., Griesinger, C., Jovin, T. M., and Zweckstetter, M. (2005) Structural characterization of copper(II) binding to α-synuclein: Insights into the bioinorganic chemistry of Parkinson's disease, *Proc. Natl. Acad. Sci. U.S.A. 102*, 1430−1435.
35. Choi, W., Zibaee, S., Jakes, R., Serpell, L. C., Davletov, B., Crowther, R. A., and Goedert, M. (2004) Mutation E46K increases phospholipid binding and assembly into filaments of human α-synuclein, *FEBS Lett. 576*, 363−368.
36. Greenbaum, E. A., Graves, C. L., Mishizen-Eberz, A. J., Lupoli, M. A., Lynch, D. R., Englander, S. W., Axelsen, P. H., and Giasson, B. I. (2005) The E46K mutation in α-synuclein increases amyloid fibril formation, *J. Biol. Chem. 280*, 7800−7807.
37. Giasson, B. I., Uryu, K., Trojanowski, J. Q., and Lee, V. M.-Y. (1999) Mutant and wild-type human α-synucleins assemble into elongated filaments with distinct morphologies *in vitro*, *J. Biol. Chem. 274*, 7619−7622.
38. Narhi, L., Wood, S. J., Steavenson, S., Jiang, Y., Wu, G. M., Anafi, D., Kaufman, S. A., Martin, F., Sitney, K., Denis, P., Louis, J. C., Wypych, J., Biere, A. L., and Citron, M. (1999) Both familial Parkinson's disease mutations accelerate α-synuclein aggregation, *J. Biol. Chem. 274*, 9843−9846.
39. Li, J., Uversky, V. N., and Fink, A. L. (2001) Effect of familial Parkinson's disease point mutations A30P and A53T on the structural properties, aggregation, and fibrillation of human α-synuclein, *Biochemistry 40*, 11604−11613.
40. Conway, K. A., Lee, S.-J., Rochet, J. C., Ding, T. T., Williamson, R. E., and Lansbury, P. T. (2000) Acceleration of oligomerization, not fibrillization, is a shared property of both α-synuclein mutations linked to early-onset Parkinson's disease: Implications for pathogenesis and therapy, *Proc. Natl. Acad. Sci. U.S.A. 97*, 571−576.
41. Goedert, M., Spillantini, M. G., and Davies, S. W. (1998) Filamentous nerve cell inclusions in neurodegenerative diseases, *Curr. Opin. Neurobiol. 8*, 619−632.
42. Prusiner, S. B. (2001) Shattuck lecture: Neurodegenerative diseases and prions, *N. Engl. J. Med. 344*, 1516−1526.

43. Findeis, M. A. (2000) Approaches to discovery and characterization of inhibitors of amyloid β-peptide polymerization, *Biochim. Biophys. Acta 1502*, 76−84.
44. Cashman, N. R., and Caughey, B. (2004) Prion diseases: Close to effective therapy? *Nat. Rev. Drug Discovery 3*, 874−884.
45. Heiser, V., Engemann, S., Bröcker, W., Dunkel, I., Boeddrich, A., Waelter, S., Nordhoff, E., Lurz, R., Schugardt, N., Rautenberg, S., Herhaus, C., Barnickel, G., Böttcher, H., Lehrach, H., and Wanker, E. E. (2002) Identification of benzothiazoles as potential polyglutamine aggregation inhibitors of Huntington's disease by using an automated filter retardation assay, *Proc. Natl. Acad. Sci. U.S.A. 99*, 16400−16406.
46. Pickhardt, M., Gazova, Z., von Bergen, M., Khlistunova, I., Wang, Y., Hascher, A., Mandelkow, E. M., Biernat, J., and Mandelkow, E. (2005) Anthraquinones inhibit tau aggregation and dissolve Alzheimer's paired helical filaments *in vitro* and in cells, *J. Biol. Chem. 280*, 3628−3635.
47. Taniguchi, S., Suzuki, N., Masuda, M., Hisanaga, S.-I., Iwatsubo, T., Goedert, M., and Hasegawa, M. (2005) Inhibition of heparin-induced tau filament formation by phenothiazines, polyphenols, and porphyrins, *J. Biol. Chem. 280*, 7614−7623.
48. Conway, K. A., Rochet, J. C., Bieganski, R. M., and Lansbury, P. T. (2001) Kinetic stabilization of the α-synuclein protofibril by a dopamine-α-synuclein adduct, *Science 294*, 1346−1349.
49. Norris, E. H., Giasson, B. I., Hodara, R., Xu, S., Trojanowski, J. Q., Ischiropoulos, H., and Lee, V. M.-Y. (2005) Reversible inhibition of α-synuclein fibrillization by dopaminochrome-mediated conformational alterations, *J. Biol. Chem. 280*, 21212−21219.
50. Cappai, R., Leck, S.-L., Tew, D. J., Williamson, N. A., Smith, D. P., Galatis, D., Sharples, R. A., Curtain, C. C., Ali, F. E., Cherny, R. A., Culvenor, J. G., Bottomley, S. P., Masters, C. L., Barnham, K. J., and Hill, A. F. (2005) Dopamine promotes α-synuclein aggregation into SDS-resistant soluble oligomers via a distinct folding pathway, *FASEB J. 19*, 1377−1379.
51. Zhu, M., Rajamani, S., Kaylor, J., Han, S., Zhou, F., and Fink, A. L. (2004) The flavonoid baicalein inhibits fibrillation of α-synuclein and disaggregates existing fibrils, *J. Biol. Chem. 279*, 26846−26857.
52. Lee, E.-N., Cho, H.-J., Lee, C.-H., Lee, D., Chung, K. C., and Paik, S. R. (2004) Phthalocyanine tetrasulfonates affect the amyloid formation and cytotoxicity of α-synuclein, *Biochemistry 43*, 3704−3715.
53. Li, J., Zhu, M., Rajamani, S., Uversky, V. N., and Fink, A. L. (2004) Rifampicin inhibits α-synuclein fibrillation and disaggregates fibrils, *Chem. Biol. 11*, 1513−1521.
54. Nonaka, T., Iwatsubo, T., and Hasegawa, M. (2005) Ubiquitination of α-synuclein, *Biochemistry 44*, 361−368.
55. Masuda, M., Dohmae, N., Nonaka, T., Oikawa, T., Hisanaga, S. I., Goedert, M., and Hasegawa, M. (2006) Cysteine misincorporation in bacterially expressed human α-synuclein, *FEBS Lett. 580*, 1775−1779.
56. Naiki, H., and Nakakuki, K. (1996) First-order kinetic model of Alzheimer's β-amyloid fibril extension in vitro, *Lab. Invest. 74*, 374−383.
57. Goedert, M., Spillantini, M. G., Jakes, R., Rutherford, D., and Crowther, R. A. (1989) Multiple isoforms of human microtubule-associated protein tau: sequences and localization in neurofibrillary tangles of Alzheimer's disease, *Neuron 3*, 519−526.
58. Hasegawa, M., Smith, M. J., and Goedert, M. (1998) Tau proteins with FTDP-17 mutations have a reduced ability to promote microtubule assembly, *FEBS Lett. 437*, 207−210.
59. Ding, T. T., Lee, S.-J., Rochet, J. C., and Lansbury, P. T. (2002) Annular α-synuclein protofibrils are produced when spherical protofibrils are incubated in solution or bound to brain-derived membranes, *Biochemistry 41*, 10209−10217.
60. Mandel, S., and Youdim, B. H. (2004) Catechin polyphenols: Neurodegeneration and neuroprotection in neurodegenerative diseases, *Free Radical Biol. Med. 37*, 304−317.
61. Lorenzo, A., and Yankner, B. A. (1994) β-Amyloid neurotoxicity requires fibril formation and is inhibited by congo red, *Proc. Natl. Acad. Sci. U.S.A. 91*, 12243−12247.
62. Esler, W. P., Stimson, E. R., Ghilardi, J. R., Felix, A. M., Lu, Y.-A., Vinters, H. V., Mantyh, P. W., and Maggio, J. E. (1997) Aβ deposition inhibitor screen using synthetic amyloid, *Nat. Biotechnol. 15*, 258−263.
63. Caughey, B., and Race, R. E. (1992) Potent inhibition of scrapie-associated PrP accumulation by congo red, *J. Neurochem. 59*, 768−771.
64. Caughey, B., Ernest, D., and Race, R. E. (1993) Congo red inhibition of scrapie agent replication, *J. Virol. 67*, 6270−6272.
65. Heiser, V., Scherzinger, E., Boeddrich, A., Nordhoff, E., Lurz, R., Schugardt, N., Lehrach, H., and Wanker, E. E. (2000) Inhibition of huntingtin fibrillogenesis by specific antibodies and small molecules: Implications for Huntington's disease therapy, *Proc. Natl. Acad. Sci. U.S.A. 97*, 6739−6744.
66. Sánchez, I., Mahlke, C., and Yuan, J. (2003) Pivotal role of oligomerization in expanded polyglutamine neurodegenerative disorders, *Nature 421*, 373−379.
67. Skovronsky, D. M., Zhang, B., Kung, M.-P., Kung, H. F., Trojanowski, J. Q., and Lee, V. M.-Y. (2000) *In vivo* detection of amyloid plaques in a mouse model of Alzheimer's disease, *Proc. Natl. Acad. Sci. U.S.A. 97*, 7609−7614.
68. Sato, K., Higuchi, M., Iwata, N., Saito, T. C., and Sasamoto, K. (2004) Fluoro-substituted and ^{13}C-labeled styrylbenzene derivatives for detecting brain amyloid plaques, *Eur. J. Med. Chem. 39*, 573−578.
69. Higuchi, M., Iwata, N., Matsuba, Y., Sato, K., Sasamoto, K., and Saido, T. C. (2005) ^{19}F and ^{1}H MRI detection of amyloid β plaques *in vivo*, *Nat. Neurosci. 8*, 527−533.
70. Schmidt, M. L., Schuck, T., Sheridan, S., Kung, M.-P., Kung, H., Zhuang, Z.-P., Bergeron, C., Lamarche, J. S., Skovronsky, D., Giasson, B. I., Lee, V. M.-Y., and Trojanowski, J. Q. (2001) The fluorescent Congo red derivative, (trans,trans)-1-bromo-2,5-bis-(3-hydroxycarbonyl-4-hydroxy)styrylbenzene (BSB), labels diverse β-pleated sheet structures in postmortem human neurodegenerative disease brains, *Am. J. Pathol. 159*, 937−943.
71. Kayed, R., Head, E., Thompson, J. L., McIntire, T. M., Milton, S. C., Cotman, C. W., and Glabe, C. G. (2003) Common structure of soluble amyloid oligomers implies common mechanism of pathogenesis, *Science 300*, 486−489.
72. Emadi, S., Liu, R., Yuan, B., Schulz, P., McAllister, C., Lyubchenko, Y., Messer, A., and Sierks, M. R. (2004) Single chain variable fragments against β-amyloid (Aβ) can inhibit Aβ aggregation and prevent Aβ-induced neurotoxicity, *Biochemistry 43*, 2871−2878.
73. Dedmon, M. W., Christodoulou, J., Wilson, M. R., and Dobson, C. M. (2005) Heat shock protein 70 inhibits α-synuclein fibril formation via preferential binding to prefibrillar species, *J. Biol. Chem. 280*, 14733−14740.
74. El-Agnaf, O. M. A., Jakes, R., Curran, M. D., Middleton, D., Ingenito, R., Bianchi, E., Pessi, A., Neill, D., and Wallace, D. (1998) Aggregates from mutant and wild-type α-synuclein proteins and NAC peptide induce apoptotic cell death in human neuroblastoma cells by formation of β-sheet and amyloid-like filaments, *FEBS Lett. 440*, 71−75.
75. Volles, M. J., and Lansbury, P. T. (2003) Zeroing in on the pathogenic form of α-synuclein and its mechanism of neurotoxicity in Parkinson's disease, *Biochemistry 42*, 7871−7878.
76. Giasson, B. I., and Lee, V. M.-Y. (2003) Are ubiquitination pathways central to Parkinson's disease? *Cell 114*, 1−8.
77. Chen, L., and Feany, M. B. (2005) α-Synuclein phosphorylation controls neurotoxicity and inclusion formation in a *Drosophila* model of Parkinson disease, *Nat. Neurosci. 8*, 657−663.

BI0600749

FEBS Letters 580 (2006) 1775–1779

Cysteine misincorporation in bacterially expressed human α-synuclein

Masami Masuda[a,b], Naoshi Dohmae[c], Takashi Nonaka[a], Takayuki Oikawa[a,b], Shin-ichi Hisanaga[b], Michel Goedert[d], Masato Hasegawa[a,*]

[a] *Department of Molecular Neurobiology, Tokyo Institute of Psychiatry, 2-1-8 Kamikitazawa, Setagaya-ku 156-8585, Tokyo, Japan*
[b] *Molecular Neuroscience Laboratory, Graduate School of Science, Tokyo Metropolitan University, 1-1 Minami-Osawa, Hachioji-shi 192-0397, Tokyo, Japan*
[c] *Biomolecular Characterization, RIKEN, 2-1 Hirosawa, Wako-Shi 351-0198, Saitama, Japan*
[d] *Medical Research Council Laboratory of Molecular Biology, Hills Road, Cambridge CB2 2QH, UK*

Received 27 January 2006; accepted 14 February 2006

Available online 24 February 2006

Edited by Jesus Avila

Abstract Bacterially expressed human α-synuclein (α-syn) has been widely used in structural and functional studies. Here we show that ~20% of human α-syn expressed in *Escherichia coli* is mistranslated and that a Cys residue is incorporated at position 136 instead of a Tyr. Site-directed mutagenesis of codon 136 (TAC to TAT) resulted in the expression of α-syn lacking Cys. Although wild-type (Y136-TAC and Y136-TAT) and mutant (C136-TGC) α-syn had similar propensities to assemble into filaments, the levels of dimeric α-syn were increased by misincorporation. To avoid potential artefacts, we recommend use of the Y136-TAT construct for the expression of human α-syn.

Keywords: α-Synuclein; Mistranslation; Cysteine; Dimerization; Aggregation

1. Introduction

Filamentous α-synuclein (α-syn) inclusions in nerve cells or glial cells are the defining neuropathological feature of a group of neurodegenerative diseases which includes Parkinson's disease (PD), dementia with Lewy bodies (DLB) and multiple system atrophy (MSA) [1]. In these so-called "α-synucleinopathies", α-syn is deposited in a hyperphosphorylated and partially ubiquitinated form [2,3]. Missense mutations (A30P, E46K and A53T) in the α-syn gene cause familial forms of PD and DLB [4–6]. Furthermore, multiplications (duplication and triplication) of a region on the long arm of chromosome 4 that encompasses the α-syn gene cause an inherited form of PD-dementia [7], indicating that the simple overproduction of wild-type α-syn is sufficient to cause disease.

Recombinant α-syn readily assembles into filaments that share many of the morphological and biochemical characteristics of the filaments present in human brain [8]. Mutations E46K and A53T in α-syn have been found to accelerate the rate of filament assembly [9,10]. Mutation A30P has been reported to increase the total aggregation of α-syn, but to slow the rate of mature filament formation [10].

The precise chain of events leading from soluble, monomeric to insoluble, filamentous α-syn is not known. Biophysical studies have suggested that dimerization of α-syn is a rate-limiting step in aggregation [11]. Human α-syn does not contain any Cys residues and hence, covalent aggregate formation caused by oxidation is restricted to dityrosine cross-links [12].

Here we report the unexpected finding that bacterially expressed human α-syn contains a significant amount of Cys. Analysis of dimeric α-syn showed that ~20% of the recombinant protein was mistranslated, with Cys at position 136 instead of Tyr. Mutagenesis of codon 136 from TAC to TAT resulted in the expression of α-syn lacking Cys. The ability of Y136C α-syn to assemble into filaments was not changed significantly. However, dimerization of the mutated protein was significantly enhanced.

2. Experimental procedures

2.1. Expression and purification of wild-type and mutant human α-syn

Human α-syn cDNA in bacterial expression plasmid pRK172 was used [13]. Codon 136 was changed from TAC to TAT or TGC by site-directed mutagenesis (Stratagene) (Fig. 1). All constructs were verified by DNA sequencing. Wild-type and mutant proteins were expressed in *Escherichia coli* BL21 (DE3) cells and purified using boiling, Q-Sepharose ion exchange chromatography and ammonium sulfate precipitation. α-Syn proteins were dialyzed against 30 mM Tris–HCl, pH 7.5, and cleared using a 20 min centrifugation at 113000 × *g*. Following separation by reverse phase high-performance liquid chromatography (RP-HPLC, Aquapore RP300 column), the absorbance at 215 nm was measured and compared with that of α-syn of known concentration, to give the concentration of the freshly purified protein.

2.2. Analysis of monomeric and dimeric α-syn by mass spectrometry

α-Syn (6 mg/ml) was incubated for 7 days at 37 °C in 30 mM Tris–HCl, pH 7.5, containing 0.02% sodium azide. Following a 20 min centrifugation at 113000 × *g*, the supernatant was fractionated on a Superdex 200 gel filtration column (10 × 300 mm, Amersham Bioscience) in 10 mM Tris–HCl, pH 7.5, containing

*Corresponding author. Fax: +81 3 3329 8035.
E-mail address: masato@prit.go.jp (M. Hasegawa).

Abbreviations: α-syn, α-synuclein; PD, Parkinson's disease; DLB, dementia with Lewy bodies; MSA, multiple system atrophy; ThS, thioflavin S; RP-HPLC, reverse phase high-performance liquid chromatography; MALDI-TOF/MS, matrix-assisted laser desorption ionization-time of flight/mass spectrometry

0014-5793/$32.00
doi:10.1016/j.febslet.2006.02.032

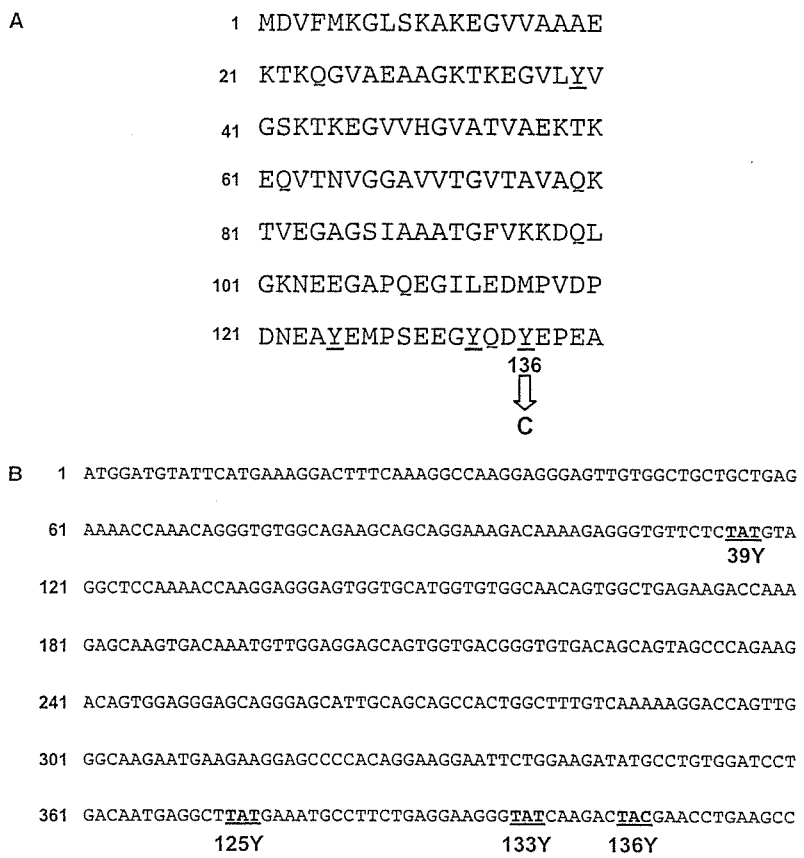

Fig. 1. Amino acid sequence (A) and cDNA sequence (B) of human α-syn. The four Tyr residues at positions 39, 125, 133 and 136 are highlighted. TAT codes for 39Y, 125Y and 133Y, whereas TAC encodes 136Y. During bacterial expression, a Cys residue is misincorporated at position 136 in a substantial fraction of α-syn.

0.15 M NaCl. The fractions were analyzed by SDS–PAGE with or without 2-mercaptoethanol (2ME) and analyzed by matrix-assisted laser desorption ionization-time of flight/mass spectrometry (MALDI-TOF/MS) using a Voyager-DE Pro mass spectrometer (PerSeptive Biosystems). Monomeric and dimeric α-syn was digested with TPCK-trypsin (Worthington Biochemical Company) for 18 h at 37 °C at an enzyme to substrate ratio of 1:20, separated by RP-HPLC on a Superspher Select B column (2.1 × 125 mm, Merck) and analyzed by mass spectrometry. The carboxy-terminal α-syn peptide was further digested for 18 h at 37 °C with V8 protease (Sigma) at an enzyme to substrate ratio of 1:10, followed by RP-HPLC. The separated tryptic-V8 peptide was then reduced for 1 h at 37 °C with 0.5% dithiothreitol (DTT) in 0.5 M Tris–HCl, pH 8.5, desalted using ZipTipC18 and analyzed by MALDI-TOF/TOF mass spectrometry using an Ultraflex (Bruker Daltonik GmbH) in a LIFT mode [14], with α-cyano hydroxyl cinnamic acid as a matrix.

2.3. Reduction and S-carboxymethylation of α-syn

Recombinant Y136-TAC and Y136-TAT α-syn (100 μg) was reduced for 1.5 h at room temperature with 1 mg DTT in 50 μl of 0.5 M Tris–HCl, pH 8.5, containing 7 M guanidine hydrochloride. Iodoacetic acid (2.5 mg) was added, followed by a 30 min incubation in the dark. The reaction mixture was then dialyzed against 30 mM Tris–HCl, pH 7.5, digested for 2 h at 37 °C with TPCK-trypsin at an enzyme to substrate ratio of 1:20 and separated by RP-HPLC.

2.4. Filament assembly of Cys-containing α-syn

Recombinant human α-syn (1 mg/ml) was incubated with shaking (200 rpm) for 96 h at 37 °C in 50 μl of 30 mM Tris–HCl, pH 7.5, containing 0.02% sodium azide. For a quantitative assessment of filament formation, the amounts of sarkosyl-insoluble α-syn and the levels of thioflavin S (ThS) fluorescence were measured as described [15].

3. Results

3.1. Identification of Cys-containing α-syn

Recombinant α-syn was incubated for 7 days at 37 °C, and fractioned by gel filtration chromatography. Two protein peaks were observed, which corresponded to monomeric and dimeric α-syn, respectively. Dimer formation was not observed in the presence of 2ME (Fig. 2A). Analysis of the monomer fraction (peak 1) by MALDI-TOF/MS gave one major signal corresponding to a molecular mass of 14460 (identical to the calculated molecular mass of monomeric human α-syn) (Fig. 2B). Analysis of the dimer fraction (peak 2) gave a signal of molecular mass 28799 (identical to the calculated molecular mass of dimeric α-syn minus 121) (Fig. 2C). To analyze this difference further, we compared the peptide maps of the tryptic digests of monomeric and dimeric α-syn. We found that the carboxy-terminal region of α-syn was modified in the dimer (see supplementary material). To identify the site of dimerization, the carboxy-terminal tryptic peptide was digested with V8 protease,

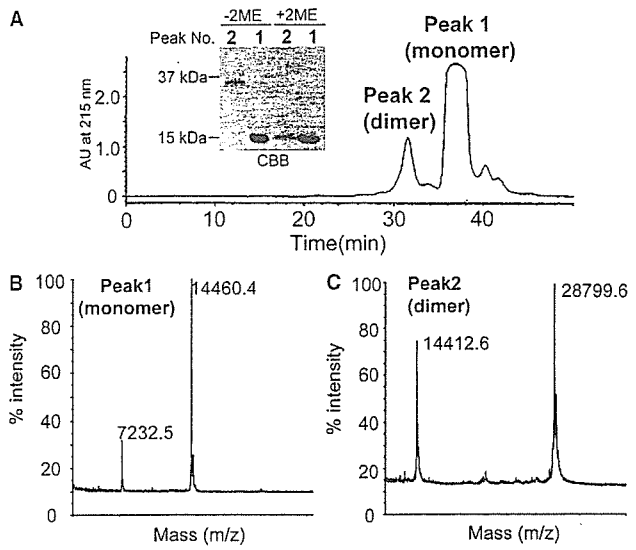

Fig. 2. Analysis of monomeric and dimeric α-syn. (A), Bacterially expressed α-syn was incubated for 7 days at 37 °C. Following ultracentrifugation, the supernatant was fractionated by gel filtration chromatography and peak 1 (monomer) and peak 2 (dimer) were run on SDS–PAGE in the absence and the presence of 2ME and visualized with Coomassie brilliant blue (CBB). (B,C), MALDI-TOF mass spectrometry analysis of peaks 1 and 2.

purified by RP-HPLC, reduced with DTT and analyzed by MALDI-TOF/TOF mass spectrometry. The product ion spectra derived from fragmentation of the charged ion at *m/z* 1011.4 resulted in a series of b and y sequence ions corresponding to the peptide GYQDCEPEA (Fig. 3). This peptide is identical to residues 132–140 of α-syn, with the exception of residue 136, which is Cys instead of Tyr. The difference between predicted and true mass of the dimer (121) could be accounted for by the mass difference between Tyr (163) and Cys (103).

3.2. Mutagenesis of codon 136 (TAC to TAT) of α-syn prevents the misincorporation of cysteine

Human α-syn contains four Tyr residues (at positions 39, 125, 133 and 136) (Fig. 1A). Tyr 136 is encoded by TAC, whereas the other three are encoded by TAT (Fig. 1B). We therefore mutated codon 136 from TAC to TAT, and found that Y136-TAC, but not Y136-TAT α-syn dimerised in the absence of 2ME (Fig. 4A). MALDI-TOF/MS analysis gave a major signal at 14460 and no signal corresponding to Cys-containing α-syn. Carboxymethylation of α-syn with codons TAC and TAT at position 136 was then used to identify the presence of Cys (Fig. 4B and C). The peptide maps of α-syn with codon TAC showed that carboxymethylation generated an extra peak at 16.7 min (arrowed in Fig. 4B). MALDI-TOF/MS and LC/MS analyses confirmed that this peak corresponded to the peptide with carboxymethylated Cys. The ratio of the peak area of carboxymethylated (16.7 min) to non-carboxymethylated (16.9 min) peptide was 1:4–5, indicating that 20–25% of recombinant α-syn carried the Y136C substitution (Fig. 4B). By contrast, when the peptide maps of α-syn with codon TAT before and after carboxymethylation were compared, no significant differences were observed (Fig. 4C). MALDI-TOF/MS and LC/MS analyses confirmed the absence of Cys and carboxymethylated Cys-containing peptides.

3.3. Filament formation of Y136-TAC, Y136-TAT and C136-TGC α-syn

Purified Y136 (TAC or TAT) and C136 α-syn were incubated for 96 h at 37 °C with agitation. Aliquots were removed daily and filament formation assessed by quantifying the level of sarkosyl-insoluble α-syn. All three proteins showed a similar

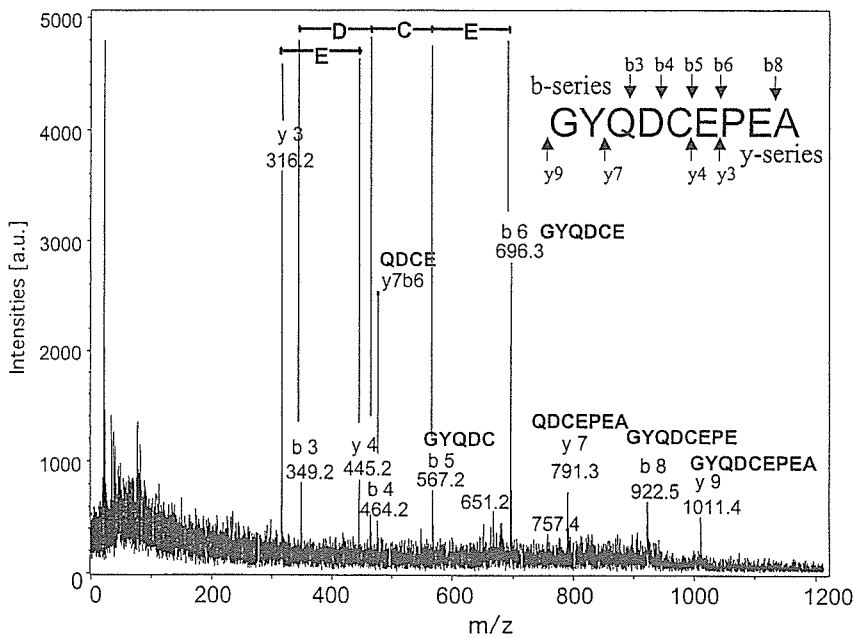

Fig. 3. MALDI-TOF/TOF mass spectrometry analysis of the dimeric peptide following digestion with V8 protease. The dimeric carboxy-terminal peptide (residues 103–140) was digested with V8 protease, purified by RP-HPLC, reduced with DTT and analyzed by MALDI-TOF/TOF mass spectrometry. The product ion spectra derived from fragmentation of the charged ion at *m/z* 1011.4 resulted in a series of b and y sequence ions, which corresponded to the peptide GYQDCEPEA (residues 132–140 of α-syn, with a Y136C mutation).

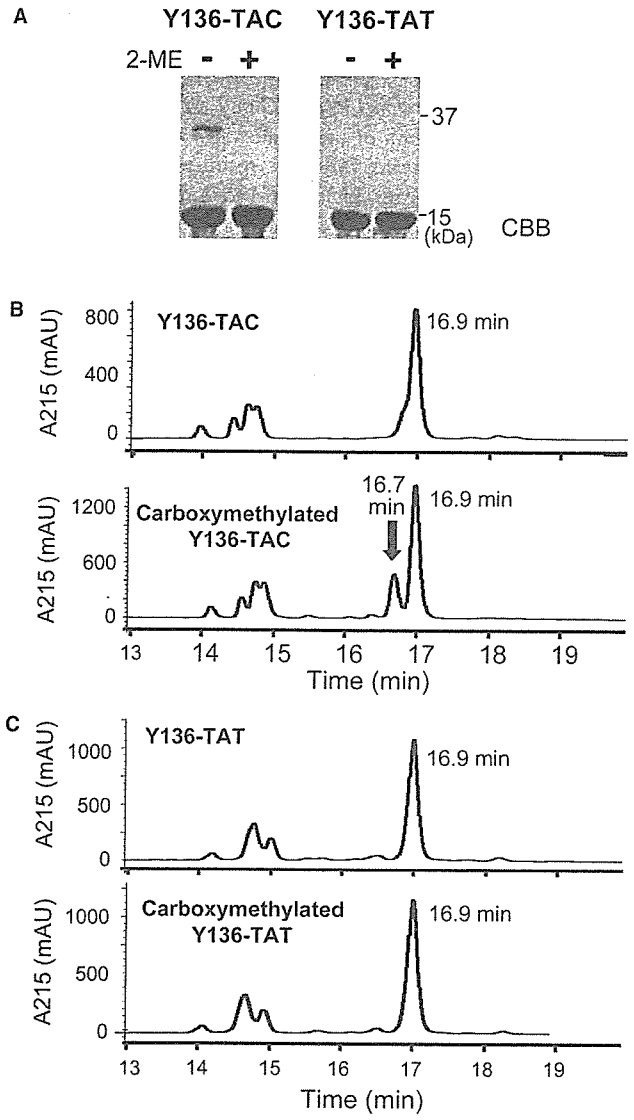

Fig. 4. Mutagenesis of codon Y136 of α-syn prevents the misincorporation of Cys. (A) α-Syn (Y136-TAC and Y136-TAT) was run on SDS–PAGE in the absence (−) and the presence (+) of 2ME and stained with CBB. (B,C), Wild-type α-syn (Y136-TAC and Y136-TAT) was carboxymethylated, digested with trypsin and separated by RP-HPLC. Separation profiles of the tryptic digests Y136-TAC (B) and Y136-TAT (C) α-syn before and after carboxymethylation. Cys-containing peptide was detected in Y136-TAC, but not Y136-TAT, α-syn following carboxymethylation (arrow at 16.7 min). These results were confirmed by MALDI-TOF/MS and LC/MS/MS analysis (data not shown).

propensity to assemble into filaments (Fig. 5). Similar results were obtained when filament formation was measured by ThS fluorescence (not shown).

4. Discussion

We report here that bacterial expression of human α-syn results in the misincorporation of Cys instead of Tyr at position 136 in 20–25% of the material. Cys-containing α-syn was found to dimerize through disulfide bond formation. Tyr 136 is encoded by TAC, unlike the other three Tyr residues in human α-syn (at positions 39, 125 and 133), which are encoded by TAT. Mutagenesis of codon 136 from TAC to TAT resulted in the expression of α-syn lacking Cys. These findings are reminiscent of protein 0.3 of bacteriophage T7, for which misincorporation of Cys instead of Tyr (one out of four Tyr residues) was observed upon bacterial expression [16]. Like codon 136 of human α-syn, Tyr 15 of protein 0.3 is encoded by TAC, which is followed by GAA in the sequence. This suggests that the misincorporation of Cys in protein 0.3 and in α-syn may have resulted from a combination of codon usage and sequence context. It remains to be seen whether the same is true of other recombinantly expressed proteins.

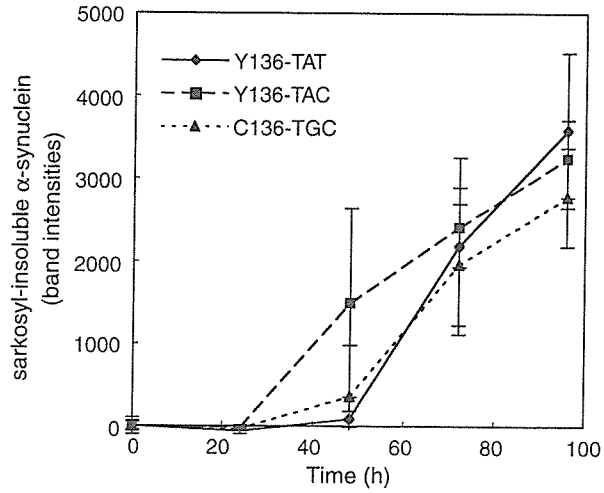

Fig. 5. Filament formation of Y136-TAC, Y136-TAT and C136-TGC α-syn. Recombinant α-syn (70 μM) was incubated with shaking. Filament formation was monitored by measuring the levels of sarkosyl-insoluble α-syn. The results are expressed as means ± S.E.M. ($n = 3$).

Recombinant α-syn is widely used for studying the protein's normal function and its abnormal assembly into filaments. Multimerization is believed to be an early step in the assembly of α-syn. We compared the ability of α-syn with Y136, C136 and a mixture of Y136 and C136 to assemble into filaments in vitro. All three protein preparations formed similar numbers of filaments with similar kinetics, as assessed by the amounts of sarkosyl-insoluble material and ThS fluorescence. This indicates that the presence of a Cys residue at position 136 does not significantly influence filament assembly of α-syn in vitro. It agrees with a recent study, which concluded that inclusion formation of α-syn was increased for mutations Y39C and Y125C, but not for mutations Y133C and Y136C [17].

In conclusion, the present findings show that a substantial proportion of bacterially expressed human α-syn carries a Tyr to Cys change at position 136. Dimerization of α-syn was significantly increased by the Cys miscorporation. This unexpected difficulty, which may well give rise to artefactual findings, can be avoided by expressing recombinant α-syn from a construct, where codon 136 has been mutated from TAC to TAT.

Acknowledgment: We thank M. Mikami for assistance with the analysis of SDS–PAGE.

Appendix A. Supplementary material

Supplementary data associated with this article can be found, in the online version, at doi:10.1016/j.febslet.2006.02.032.